Hes·so VALAIS WALLIS
School of Engineering

DCU

Hes·so
Haute Ecole Spécialisée de Suisse occidentale
Fachhochschule Westschweiz
University of Applied Sciences and Arts Western Switzerland

Degree Programme
Life Technologies

Major Biotechnology

Bachelor's thesis
Diploma 2016

Carried out in Dublin City University

Yannick Jaquet

Evaluation of Activated Alginate-GO Beads for Removal of Pharmaceuticals from Water

Professor
Prof. Dr. Fabian Fischer

Expert
Dr. Jenny Lawler

Submission date of the report
15.10.2016

HES-SO Valais-Wallis • rte du Rawyl 47 • C.P. • 1950 Sion 2
+41 27 606 85 23 • hei@hevs.ch • www.hevs.ch

Valais excellence

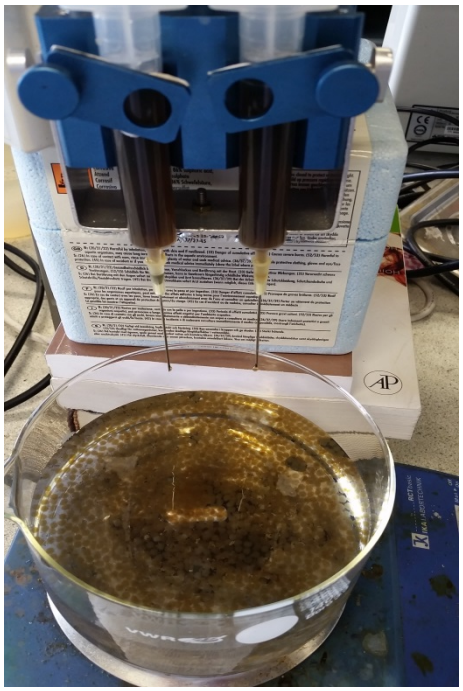

Evaluation of Activated Alginate-GO Beads for Removal of Pharmaceuticals from Water

Graduate Yannick Jaquet

Objectives

The objective is to analyse Ca-Alg_2/GO beads as an adsorbent, testing the effect of agitation time, initial concentration, pH and temperature on the adsorption of methylene blue, famotidine and diclofenac onto Ca-Alg_2 and Ca-Alg_2/GO beads.

Methods | Experiences | Results

Carbonaceous materials have attracted significant attention for applications like pollutant removal due to a high specific surface area and adsorption capacity. Among several methods available to remove pollutant from water, adsorption seems to be cheap and highly effective. Ca-Alg_2/GO beads were investigated as an adsorbent for two pharmaceuticals, Famotidine (FMTD) and Diclofenac (DFC), and a dye, Methylene Blue (MB).

The initial concentration, adsorbent dose, pH and temperature were all seen to play an important role in the adsorption. The Langmuir adsorption isotherm fitted the experimental data for each compound best, with maximum adsorption capacities of 1334, 35.50 and 36.35 $mg \cdot g^{-1}$ for MB, FMTD and DFC respectively with Ca-Alg_2/GO20. An analysis of the adsorption kinetics showed that the pseudo-second-order model fit the data for MB and FMTD and the pseudo-first-order model fit best for DFC. The adsorption was found to be exothermic and spontaneous. Desorption studies indicate that HCl 0.1 M was the best to elute MB from the beads with an efficiency up to 89%.

This project demonstrated that Ca-Alg_2/GO beads are an efficient adsorbent and could be used in drinking or wastewater treatment plants in order to reduce the concentration of hazardous organic pollutants with the potential to negatively affect the aquatic environment and human health.

Bachelor's Thesis
| 2016 |

Degree programme
Life Technologies

Field of application
Biotechnology

Supervising professor
Prof. Dr. Fabian Fischer
Fabian.Fischer@hevs.ch

Partner
Dublin City University
Dr. Jenny Lawler
jenny.lawler@dcu.ie

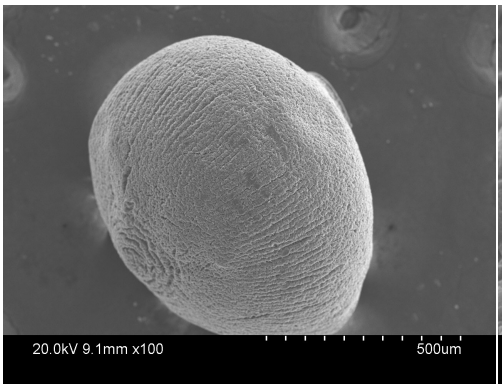

SEM image of Ca-Alg_2/GO20 dried bead, with a magnification of 100 times and an accelerating voltage of 20 kV.

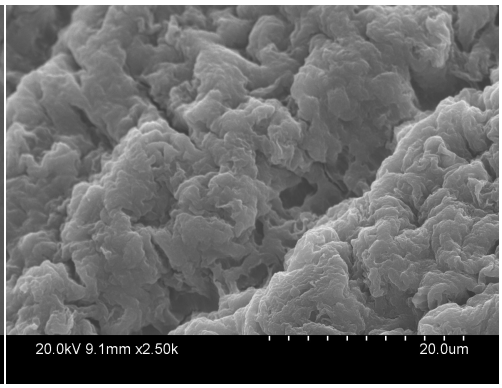

SEM image of Ca-Alg_2/GO20 dried bead, with a magnification of 2500 times and an accelerating voltage of 20 kV.

Table of contents

1 Introduction

1.1 Overview

Nowadays, agricultural, industrial and domestics purposes use more than one-third of the available freshwater on Earth. These activities lead to water pollution with an uncountable number of different compounds. Every year, about 300 million tons of synthetic compounds from industrial and consumer products, 140 million tons of fertilizers and several million tons of pesticides from agriculture are released into natural waters [1].

Thus, natural water and drinking water source contamination has become a major concern for environmental and public health. Wastewater treatment plants have been well established in developed countries, providing for the removal of contaminants in treated water such as acids, salts, nutrients or natural organic matter occurring at $\mu g \cdot L^{-1}$ to $mg \cdot L^{-1}$ (termed macropollutants). However, not every chemical is satisfactorily removed. Some of them are just partially eliminated remaining at trace concentration, meanwhile, others are not even retained [2].

These pharmaceuticals reach aquatic organisms at low to very low concentrations ($\mu g \cdot L^{-1}$ to $ng \cdot L^{-1}$). These chemicals, called micropollutants, have been found ubiquitously in the past decade and toxic effects on the environment and human being are still not well understood. It is also far more difficult to assess the threat of thousands of trace contaminants in comparison with macropollutants, which generally lead to oxygen depletion in the receiving waters due to eutrophication and algal blooms [3].

1.2 Alginate

Alginate or alginic acid is an anionic polysaccharide. It is found in the cell walls of brown algae and it is an important compound present in biofilms produced by the bacterium *Pseudomonas aeruginosa*. The structure of the alginic acid, as shown in Figure 1, is a linear copolymer of homopolymeric blocks of (1-4)-linked β-D-mannuronate (M) and α-L-guluronate (G) residues covalently linked together.

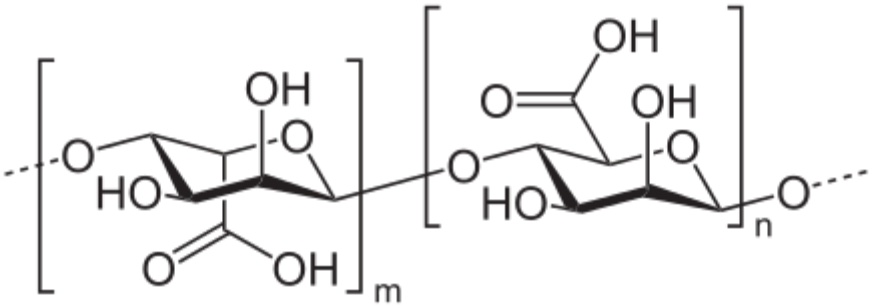

Figure 1 : Structure of alginate polymer. Guluronate residue is shown on the left and mannuronate on the right [4].

Alginate is used as thickener, setting agent, emulsifier and stabilizer in many different industrial products like food, cosmetic products, paints or inks and pharmaceuticals. Alginate beads can also be used in medicine for the encapsulation

of therapeutics or fragile biological materials (enzymes, microorganisms, human and animal cells).

Alginate is water-soluble making a liquid solution but it forms a hydrogel when mixed with divalent cations like Ca^{2+}.

Alginate chains are cross-linked with the bivalent cation from $CaCl_2$ usually to form a three-dimensional ionotropic gel. The gelation process occurs with the incorporation of Ca^{2+}-ions into the structure of guluronate residues (G blocks) [5]. This formation is known as the egg-box model (Figure 2) [6]. The gel formation and gel strength is determined by the length of the G blocks [7]. Calcium alginate beads can be applied in the treatment of water. The carboxyl groups interact with contaminants forming a complex easily separable from the water. The adsorption capacity of alginate can be improved by adding graphene oxide [8]. It is also a cheap and biocompatible polymer compared to materials with similar properties [9].

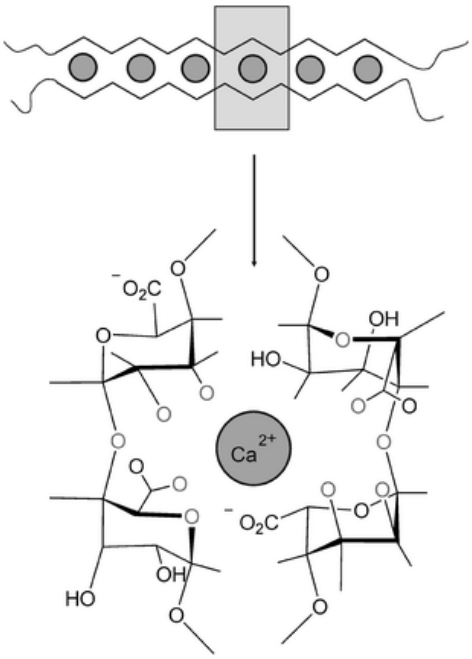

Figure 2 : Egg-box model [10]

1.3 Graphene oxide

Graphene oxide is an emerging carbon nanomaterial with mono-atom-layer structure. This is a two-dimensional compound of carbon atoms densely packed in a honeycomb framework. Figure 3 shows the structure of graphene oxide with different functional groups making part of the structure such as hydroxyl (-OH), carboxyl (-COOH), ketone (-C=O), and epoxyl (-C-O-C-).

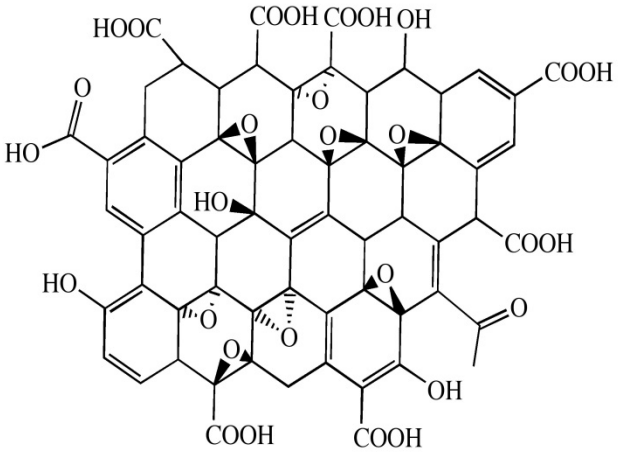

Figure 3 : Structure of graphene oxide [11]

Graphene oxide has attracted scientific interest since its discovery due to its potential applications in water treatment membranes, electronics and energy storage [12]. Graphene oxide has unique properties such as large theoretical surface area (2630 $m^2 \cdot g^{-1}$), high thermal and chemical stability, high conductivity and good mechanical flexibility [13]. This is why it shows great promise for potential applications also in technological fields like field-effect transistors [14], sensors [15], solar cells [16] and as an adsorbent for removal or sequestration of heavy metals [17], dyes [18] and pharmaceuticals [19].

The high efficiency of graphene oxide as an adsorbent is mainly due to its functional groups acting like sorption sites which interact with contaminants by electrostatic attraction, hydrogen bonding, Lewis acid-base interaction or $\pi - \pi$ stacking. GO is also interesting because it can be produced at large-scale. Furthermore, graphene

oxide is considered as an environmental friendly carbon nanomaterial [20]. However, with growing concern over the release of nanomaterials into the environment, it is desirable to encapsulate the graphene oxide in alginate in order to make it easily removable from treated water, and reusable, to avoid accumulation in the environment.

1.4 Methylene blue

Methylene blue, chemical formula $C_{16}H_{18}N_3SCl$ and molecular weight 319.85 $g \cdot mol^{-1}$, shown in the Figure 4, is a heterocyclic aromatic chemical dye. This cationic compound is one of the most used dyes in textile, paper, plastic, and cosmetic industries [21]. The major problem of these industries is the release of coloured effluent.

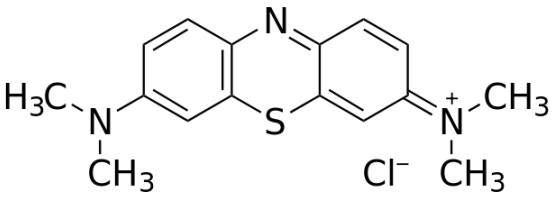

Figure 4 : Structure of methylene blue [22]

Methylene blue is not a highly toxic chemical but it can be dangerous for humans and animals by causing heart rate increase, nausea and vomiting [23]. Moreover, the dyeing water reduces the solar light penetration and retards photosynthetic activity of aquatic plants [24]. In addition, dyes are highly visible and even minor release might cause abnormal coloration of the water [25]. The waste water treatment is complicated due to complex molecular structures. These dyes cause also chemical and biological changes destroying the aquatic life by consuming dissolved oxygen or isolating metal ions producing microtoxicity to organisms [26,27].

1.5 Famotidine

The pharmaceutical famotidine is a histamine H_2-receptor antagonist. It enables the stomach to produce less acid. This is why this medicine is used to prevent and treat ulcers in the stomach and intestines. It treats also gastroesophageal reflux disease and Zollinger-Ellison syndrome (tumors in the pancreas or small intestine). Famotidine, shown in Figure 5, is a cationic chemical, its molecular formula is $C_8H_{15}N_7O_2S_3$ and its molecular weight is 337.449 $g \cdot mol^{-1}$.

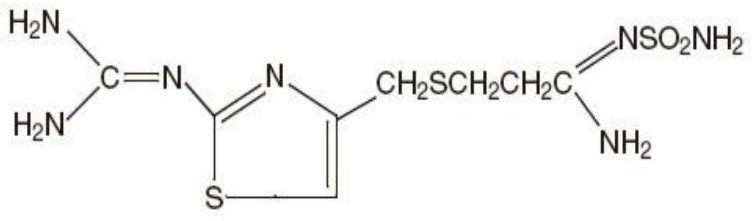

Figure 5 : Structure of famotidine [28]

Famotidine is also used for treatment of Alzheimer's and Parkinson's diseases [29,30]. In wastewater treatment plants, famotidine has been detected in 61% of wastewater samples and in 57% of wastewater effluent samples, indicating both its abundance and also the difficulty in removing it in typical WWTPs [31]. While famotidine has not been implicated in acute toxicity to freshwater crustaceans (*Thamnocephalus platyurus*) and fish (*Oryzias latipes*), other pharmaceuticals such as carbamazepine or ibuprofen were shown to affect both aquatic organisms [32]. However, potential effects of chronic toxicity due to long-term, low-level exposure to

famotidine are not known and further assessments need to be done to ascertain the effects of such chemicals.

1.6 Diclofenac

Diclofenac, $C_{14}H_{11}Cl_2NO_2$ and molecular weight of 296.149 $g \cdot mol^{-1}$, is shown in Figure 6. It is a nonsteroidal anti-inflammatory drug prescribed to reduce inflammation, pain as an analgesic and dysmenorrhea. Diclofenac consumption is associated with serious dose-dependent gastrointestinal and renal adverse effects, and increases vascular and coronary risks by about a third [33]. It was synthetized by Alfred Sallmann and Rudolf Pfister and Ciba-Geigy commercialized this chemical as Voltaren in 1973 [34]. The main mechanism of diclofenac responsible of anti-inflammatory, analgesic and antipyretic effects is the inhibition of prostaglandin synthesis by inhibiting the cyclooxygenase (COX).

In wastewater treatment plants, the frequency of detection of diclofenac is 96, 86 and 93 % in wastewater influent, wastewater effluent and river water respectively [31]. Several studies were conducted in order to investigate the toxic effects of diclofenac on aquatic environment. The investigations showed that cytological alterations in liver, kidney and gills of rainbow trout (*Oncorhynchus mykiss*) were already observed at a concentration of 1 $\mu g \cdot L^{-1}$ of diclofenac [36]. Diclofenac exposure to trout has been shown to induce severe glomerulonephritis resulting into kidney failure [37].

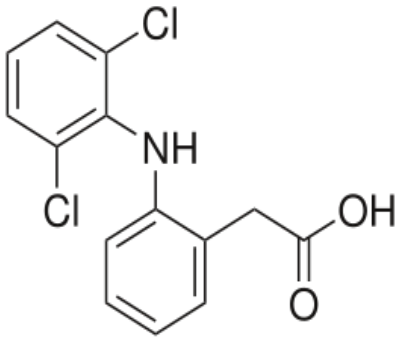

Figure 6 : Structure of diclofenac [35]

1.7 Removal techniques

Many different treatment techniques have been developed for the removal of dyes and pharmaceuticals from water. Flocculation, ozonation, chemical and biological degradation, precipitation, membrane filtration, ion exchange or coagulation are all examples of techniques available to eliminate pollutants [38-40]. These technologies possess their own disadvantages leading to the drive for research into new approaches. Among them, adsorption shows high efficiency while it's utilization is simple and cheap. Carbonaceous material as adsorbents are very commonly used (with activated carbon being the most applied commercial adsorbent), and graphene oxide seemed promising in light of previous studies [41].

1.8 Objectives

The aim of this project was to produce calcium alginate beads with graphene oxide incorporated into the structure, in order to enhance the adsorption properties. The effects of initial concentration, adsorbent dose, pH, temperature, contact time were investigated. Adsorption kinetics and isotherms were evaluated with different models such as pseudo-first-order, pseudo-second-order, intraparticle diffusion, Langmuir and Freundlich models. In addition, thermodynamic and desorption studies were performed. Thus, Ca-Alg_2/GO beads were assessed as potential adsorbent for three micropollutants.

2 Materials and Methods

2.1 Materials

2.1.1 Chemicals

The chemicals used for the experiments were as shown below in Table 1.

Table 1 : Chemicals, suppliers and lot number

Products	Suppliers	Lot
Sodium alginic acid	Sigma Aldrich	MKBP7317V
Calcium chloride dihydrate	Fischer Chemical	1526483
Graphite flakes	Asbury Carbons	699131
Potassium permanganate	DCU	-
Sulphuric acid 95-98%	Merck	K39234613 839
Hydrogen peroxide 30%	Merck	K15118897 047
Famotidine	Sigma Aldrich	F6889
Diclofenac sodium	Sigma Aldrich	BCBN3367V
Methylene blue	Sigma Aldrich	129H3485
Hydrochloric acid 37%	Acros Organics	A0332017
Sodium hydroxide	Fisher Chemical	1294722
Ethanol absolute	Fisher Chemical	1534800

2.1.2 Equipment

- Syringe pump, Pump Supplied, model Fusion 200, Chemyx Inc.
- 700 W microwave, Sanyo
- Spectrophotometer UV/VIS, Unicam, Helios gamma
- Analytical balance, Mettler Toledo
- Magnetic stirrer, Ika Labortechnik
- pH meter, Jenway 3510
- Centrifuge, Yingtai Instrument, TG16
- Ultrasonic Cleaner, WiseClean, WUC-A02H
- Universal oven U, Memmert
- Cold and warm rooms, 5 and 30 °C
- Agar sputter coater, Agar scientific, model 108, serial n°A5600
- Scanning electron microscope, Hitachi, S-3400N

2.1.3 Preparation of HCl 0.1 M solution

HCl 0.1 M solution was prepared by pipetting 8.3 mL of hydrochloric acid 37% into a 1L volumetric flask. Then the flask was filled with deionized (DI) water. The solution was stirred until homogenization.

2.1.4 Preparation of HCl 1 M solution

HCl 1 M solution was prepared by pipetting 83 mL of hydrochloric acid 37% into a 1L volumetric flask. Then the flask was filled with deionized (DI) water. The solution was stirred until homogenization.

2.1.5 Preparation of HCl 10 % solution

HCl 10 % solution was prepared by measuring 270 mL of hydrochloric acid 37 % with a cylinder. Then it was poured into a 1 L volumetric flask and the flask was filled with DI water. The solution was stirred until homogenization.

2.1.6 Preparation of NaOH 0.1 M solution

NaOH 0.1 M solution was prepared by weighing 4.00 g of sodium hydroxide into a 1 L volumetric flask. Then 1 L of DI water was added into the flask. The solution was stirred until complete dissolution. The solution was left until the temperature reached room temperature.

2.1.1 Preparation of NaOH 1 M solution

NaOH 1 M solution was prepared by weighing 40.0 g of sodium hydroxide into a 1 L volumetric flask. Then 1 L of DI water was added into the flask. The solution was stirred until complete dissolution. The solution was left until the temperature reached room temperature.

2.1.2 Preparation of graphene oxide (GO) solution

Graphite flakes were placed in small portions in a beaker in a 700 W microwave on maximum power three times for a duration of 10 seconds to produce expanded graphite. 2 g of expanded graphite, 10 of dried potassium permanganate and 250 mL of sulphuric acid were added to a 2000 mL round bottomed flask. The mixture was stirred overnight at room temperature. 500 mL of DI water were added into the flask maintaining the temperature below 80 °C using an ice bath. Then 100 mL of hydrogen peroxide 30 % solution were added slowly to the mixture resulting in a colour change to golden brown. The mixture was stirred for 30 minutes, the resulting particles were washed with 750 mL HCl 10 % solution and centrifuged three times. Obtained graphene oxide was resuspended in 750 mL of DI water and centrifuged to remove the water three times. Purified graphene oxide was resuspended in 50 mL of DI water. In order to establish to exact concentration of graphene oxide, exactly 1 g was spread in a beaker, dried overnight at 60 °C and weighed again to find out the absolute weight of GO. 1 wt% solution was GO solution was prepared on this basis.

2.1.3 Preparation of beads

2.1.3.1 Sodium alginate solution 2 % w:v

Sodium alginate solution was prepared by weighing 5 g of sodium alginic acid into a conical flask. Then 250 mL of DI water was added into the flask. The solution was continuously agitated with a magnetic stirrer until dissolution.

2.1.3.2 Calcium chloride solution 6 % w:v

Calcium chloride solution was prepared by weighing 39.7 g of calcium chloride dihydrate into a conical flask. Then 500 mL of DI water was added into the flask. The solution was continuously agitated with a magnetic stirrer until dissolution.

2.1.3.3 Sodium alginate / Graphene oxide solutions

Na-Alg/GO solutions were prepared by weighing 5, 10 or 20 g of 1 % w/w GO concentrate into a conical flask. Then 50 mL of DI water was added into the flask. An ultra-sonication treatment was used to dissolve the graphene oxide. Afterwards, this solution was added to 250 mL of the Na-Alg solution 2 % w:w and stirred until homogenization. Na-Alg solution without graphene oxide was prepared by adding 50 mL of DI water to 250 mL of the Na-Alg solution 2 % w:w.

2.1.3.4 Ca-Alg_2, Ca-Alg_2/GO5, Ca-Alg_2/GO10, Ca-Alg_2/GO20 beads

Ca-Alg_2 beads were first prepared using the Na-Alg solution without graphene oxide and a syringe pump with a flow rate of 20 $mL \cdot min^{-1}$ and two 10 mL syringes with a 1 mm needle. The solution was dropped into an aqueous coagulation bath of $CaCl_2$ 6 % w:v at room temperature. The bath of $CaCl_2$ was continuously agitated with a magnetic stirrer in order to prevent beads agglomeration. After dropping the Na-Alg solution, the beads were left 24 hours without agitation to achieve a complete formation of Ca-Alg_2 gel beads. Then the beads were collected and washed three times with 500 mL of DI water.

The same procedure was used to prepare Ca-Alg_2/GO5, Ca-Alg_2/GO10, Ca-Alg_2/GO20 beads, except Na-Alg solutions used. The corresponding aqueous Na-Alg/GO solution was used in order to obtain the right ratio of Ca-Alg_2/GO beads. Increase in GO content above GO20 led to the stability of the beads being adversely impacted.

2.1.3.5 Activation of beads

The Ca-Alg_2, Ca-Alg_2/GO5, Ca-Alg_2/GO10, Ca-Alg_2/GO20 beads were activated with a pH 4 solution. The total amount of beads of the selected type was placed in a 600 mL beaker. To prepare the pH 4 solution, 0.1 M HCl was slowly added to DI water until reached the desired pH was reached. 400 mL of the pH 4 solution were added to each beaker. The beakers were agitated for 3 h at room temperature. Afterwards, the beads were collected, rinsed three times with 300 mL of DI water and stored in a closed bottle at room temperature.

2.1.3.6 Drying of beads

The Ca-Alg_2, Ca-Alg_2/GO5, Ca-Alg_2/GO10, Ca-Alg_2/GO20 beads were dried in an oven at 60 °C over 2 days in order to reach a constant weight. The beads were stored in plastic vials at room temperature.

2.2 Methods

2.2.1 Characterization of beads

The morphological structure of the beads was analysed by scanning electron microscopy (SEM) analysis. The Ca-Alg_2, Ca-Alg_2/GO5, Ca-Alg_2/GO10 or Ca-Alg_2/GO20 dried beads were coated with a layer of gold using a sputter coater to make them conductive. For each kind of beads, four pictures were taken with the microscope. The magnification used was 100 x, 500 x, 2500 x and 5000 x with accelerating voltage of 20 kV.

2.2.2 Effect of the initial concentration

The effect of the initial concentration was studied using 0.05 g of Ca-Alg_2, Ca-Alg_2/GO5, Ca-Alg_2/GO10 or Ca-Alg_2/GO20 dried beads. The adsorption was carried out over 24 hours to ensure equilibrium at 125 rpm at room temperature (22 °C) in 250 mL conical flask at pH 7, 7 and 2 for MB, FMTD and DFC respectively. The concentrations tested were 10, 100, 500, 1000 $mg \cdot L^{-1}$ for MB, 10, 25, 100, 250 $mg \cdot L^{-1}$ for FMTD and 1, 5, 10, 25 $mg \cdot L^{-1}$ for DFC. Then, the adsorbate final concentration was determined using a UV-VIS spectrophotometer at a wavelength of 660, 286 and 274 nm for MB, FMTD and DFC, respectively. Afterwards, the concentration was calculated using a calibration curve. The adsorbed amount at equilibrium q_{eq} ($mg \cdot g^{-1}$) was calculated using Equation 1 below.

$$q_{eq} = \frac{(C_0 - C_{eq}) \cdot V}{m_{ads}} \quad (1)$$

Where C_0 ($mg \cdot L^{-1}$) is the initial concentration, C_{eq} ($mg \cdot L^{-1}$) the equilibrium concentration, V (L) the volume of drug solution and m_{ads} (g) the adsorbent mass.

2.2.3 Effect of the adsorbent dose

The effect of the adsorbent dose was studied using 0.01, 0.025, 0.05 and 0.1 g of Ca-Alg_2, Ca-Alg_2/GO5, Ca-Alg_2/GO10 or Ca-Alg_2/GO20 dried beads. The beads were put into a 250 mL conical flask and 75 mL of MB, DFC or FMTD solution with a concentration of 10 $mg \cdot L^{-1}$ was added. The concentrations of the beads were 0.133, 0.333, 0.667 and 1.333 $g \cdot L^{-1}$. The flasks were agitated at 125 rpm, room temperature, with a pH of 7 for MB, FMTD and pH 2 for DFC over 24 hours to ensure that equilibrium was reached. The adsorbate final concentration was determined by UV-VIS at wavelengths of 660, 274 and 286 nm for MB, DFC and FMTD, respectively. The concentration was calculated using a calibration curve and the adsorbed amount at equilibrium (Equation 1).

2.2.4 Effect of the pH

To study the effect of pH, four different values of pH were tested. The adsorption was performed at pH 7, 9, 10 and 11 for MB and FMTD whereas the adsorption for DFC was made at pH 2, 3.5, 5 and 7. In order to adjust the pH and controlled by a

pH-meter, 1 M solutions of HCl or NaOH were added in the drug solutions. 0.05 g of Ca-Alg_2, Ca-Alg_2/GO5, Ca-Alg_2/GO10 or Ca-Alg_2/GO20 dried beads were put in a 250 mL conical flask with 75 mL of drug solution at 10 $mg \cdot L^{-1}$ and agitated for 24 hours at 125 rpm at room temperature. The absorbance was determined by UV-VIS. The concentration and the adsorbed amount at equilibrium were calculated as described previously.

2.2.5 Effect of the temperature

The influence of the temperature was studied by performing the adsorption process at 4, 22 and 30 °C. The adsorption was performed with 0.05 g of Ca-Alg_2, Ca-Alg_2/GO5, Ca-Alg_2/GO10 or Ca-Alg_2/GO20 dried beads in a 250 mL conical flask with 75 mL of drug solution at 10 $mg \cdot L^{-1}$ and agitated for 24 hours at 125 rpm, at pH 7 for MB and FMTD and pH 2 for DFC. Afterwards, the concentration and adsorbed amount were determined as described previously.

2.2.6 Thermodynamics studies

The thermodynamic parameters of adsorption were determined at 4, 22 and 30°C in order to evaluate the feasibility and the spontaneous nature of the adsorption. Distribution coefficient for the adsorption K_d (-), enthalpy change $\Delta H°$ ($J \cdot mol^{-1}$), entropy change $\Delta S°$ ($J \cdot K^{-1} \cdot mol^{-1}$) and Gibbs free energy change $\Delta G°$ ($J \cdot mol^{-1}$) were calculated using the following Equations 2 and 3:

$$K_d = \frac{C_i - C_{eq}}{C_{eq}} \quad (2)$$

Where C_i ($mg \cdot L^{-1}$) is the initial concentration of the solution and C_{eq} ($mg \cdot L^{-1}$) the equilibrium concentration in solution.

A plot of $Ln(K_d)$ versus 1/T gives a straight line where the slope and the intercept were used to calculate the enthalpy and entropy change using Equation 3 below.

$$Ln(K_d) = \frac{\Delta S°}{R} - \frac{\Delta H°}{RT} \quad (3)$$

Where R is the gas constant (8.345 $J \cdot mol^{-1} \cdot K^{-1}$) and T (K) is the temperature of the solution during the adsorption process.

The standard Gibbs free energy change $\Delta G°$ was obtained from Equation 4:

$$\Delta G° = \Delta H° - T\Delta S° \quad (4)$$

2.2.7 Effect of the contact time

The effect of the contact time and the kinetics parameters were studied using 0.05 g of Ca-Alg_2, Ca-Alg_2/GO5, Ca-Alg_2/GO10 or Ca-Alg_2/GO20 dried beads. The adsorption was carried out at 125 rpm at room temperature (22 °C) in 250 mL conical flask with 75 mL of drug solution at 10 $mg \cdot L^{-1}$ at pH 7, 7 and 2 for MB, FMTD and DFC respectively. Samples were taken at time 0, 30, 60, 90, 120, 150, 180, 240, 300, 360, 1380 and 1440 minutes. Then, the adsorbate concentration was determined using a UV-VIS spectrophotometer at a wavelength of 660, 286 and 274 nm for MB, FMTD and DFC, respectively. Afterwards, the concentration was calculated using a calibration curve. The adsorbate capacity q_t ($mg \cdot g^{-1}$) at time t was calculated using Equation 5.

$$q_t = \frac{(C_0 - C_t) \cdot V}{m_{ads}} \quad (5)$$

Where C_0 ($mg \cdot L^{-1}$) is the initial concentration, C_t ($mg \cdot L^{-1}$) the concentration at time t, V (L) the volume of drug solution and m_{ads} (g) the adsorbent mass.

2.2.8 Kinetics

The three most common models were used to fit the experimental data of this work. The linearized-integral form of the pseudo-first-order Lagergren equation is shown in Equation 6 below.

$$ln(q_{eq} - q_t) = ln(q_{eq}) - k_1 \cdot t \quad (6)$$

Where k_1 (min^{-1}) is the Lagergren rate constant, q_{eq} ($mg \cdot g^{-1}$) is the maximum adsorbed amount at equilibrium, and q_t ($mg \cdot g^{-1}$) is the amount of adsorption at time t (min). The values of k_1 and q_{eq} were determined from the intercept and the slope of a plot of $\ln(q_{eq} - q_t)$ versus t.

The linearized-integral form of the pseudo-second-order model is shown in Equation 7 below.

$$\frac{t}{q_t} = \frac{1}{k_2 \cdot q_{eq}^2} - \frac{1}{q_{eq}} \cdot t \quad (7)$$

Where k_2 ($g \cdot mg^{-1} \cdot min^{-1}$) is the pseudo second-order rate constant of adsorption. The parameters k_2 and q_{eq} were determined from the intercept and the slope of a plot of t/q_t versus t.

The last model is the intraparticle diffusion model represented in Equation 8 below.

$$q_t = k_{ip} \cdot t^{1/2} + C_{ip} \quad (8)$$

Where k_{ip} ($mg \cdot g^{-1} \cdot min^{-0.5}$) is an intraparticle diffusion rate constant and C_{ip} ($mg \cdot g^{-1}$) is related to the thickness of the diffusion boundary layer. These parameters were obtained from a plot of q_t versus $t^{1/2}$.

2.2.9 Adsorption isotherms

Two mathematical models have been used to describe the adsorption process. The Langmuir model and the Freundlich model were selected because they are the most commonly used models to study the adsorption equilibrium. The Langmuir equation is as follows in Equation 9 [42].

$$q_{eq} = q_{max} \cdot \frac{C_{eq}}{k_L + C_{eq}} \quad (9)$$

Where q_{max} ($mg \cdot g^{-1}$) is the maximum adsorption capacity corresponding to complete monolayer coverage, C_{eq} ($mg \cdot L^{-1}$) is the concentration at equilibrium in the solution and k_L ($L \cdot g^{-1}$) is a constant related to adsorption capacity and energy of adsorption.

The Freundlich equation is an empirical model based on the adsorption on a heterogeneous surface. The Freundlich model is shown in Equation 10 [43].

$$q_{eq} = k_F \cdot C^n \quad (10)$$

Where k_F ($L \cdot g^{-1}$) and n (-) are the Freundlich constants, indicating the adsorption capacity and the adsorption intensity, respectively.
In order to determine the constants of Langmuir and Freundlich, Excel Solver was used to fit the adsorption isotherm models with the experimental data. The sum of squared differences between experimental q_{eq} and calculated q_{eq} was minimized by changing the constants of the models with the solver to find the best non-linear regression.

2.2.10 Desorption

The adsorption batch was performed using 0.05 g of Ca-Alg_2, Ca-Alg_2/GO5, Ca-Alg_2/GO10 or Ca-Alg_2/GO20 dried beads. The adsorption was carried out over 24 hours to ensure equilibrium at 125 rpm at room temperature in 250 mL conical flask with 75 mL of drug solution at 10 $m \cdot L^{-1}$ at pH 7, 7 and 2 for MB, FMTD and DFC respectively. Afterwards, the concentration at equilibrium was determined, the solution was removed and the beads were washed three times with deionized water. The desorption of the beads was studied using three different chemicals, HCl 0.1 M, NaCl 1 M and ethanol 1% v/v. The desorption process was carried out in 250 mL conical flasks with 75 mL of removal solution at room temperature. The conical flasks were agitated for 24 hours at 125 rpm. Then, the final concentration in solution was determined using a UV-VIS spectrophotometer at a wavelength of 660, 286 and 274 nm for MB, FMTD and DFC, respectively. The percentage of desorption was calculated by the Equation 11 below.

$$Desorption = \frac{(q_{eq,a} - q_{eq,d})}{q_{eq,a}} \cdot 100 \quad (11)$$

Where $q_{eq,d}$ ($mg \cdot g^{-1}$) is the adsorbed amount at equilibrium after 24 hours of desorption, $q_{eq,a}$ ($mg \cdot g^{-1}$) is the adsorbed amount at equilibrium after 24 hours of adsorption.

3 Results

3.1 Characterization of beads

SEM analysis was carried out in order to analyse and characterize the morphological structure of the beads. SEM images, with a magnification of 500 and 5000 times, of Ca-Alg_2, Ca-Alg_2/GO5, Ca-Alg_2/GO10 or Ca-Alg_2/GO20 dried beads are shown in Figures 7 and 8 below.

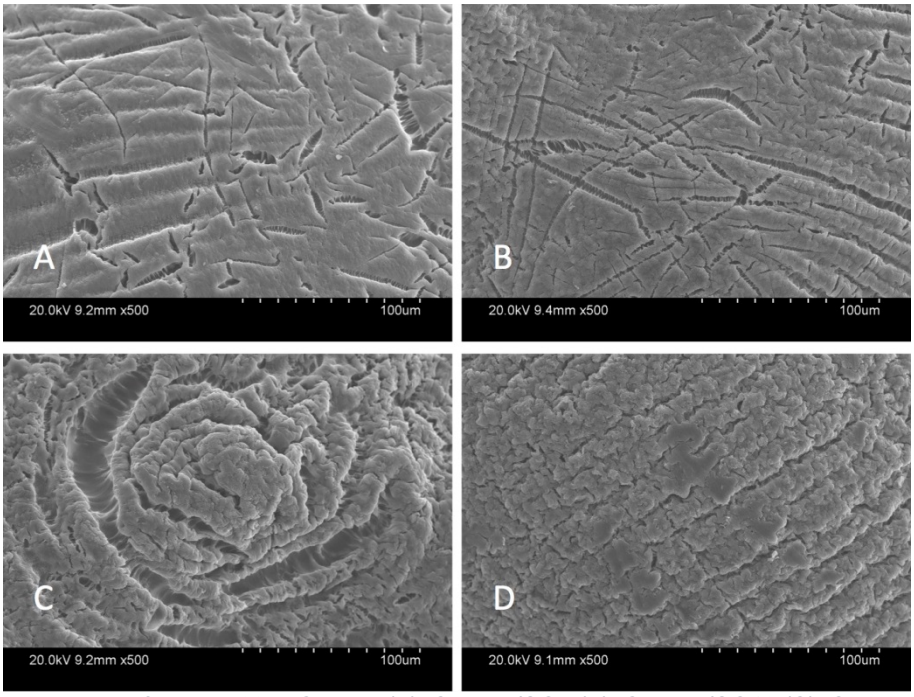

Figure 7 : SEM images, magnification 500 x, Ca-Alg_2 (A), Ca-Alg_2/GO5 (B), Ca-Alg_2/GO10 (C), Ca-Alg_2/GO20 (D) beads

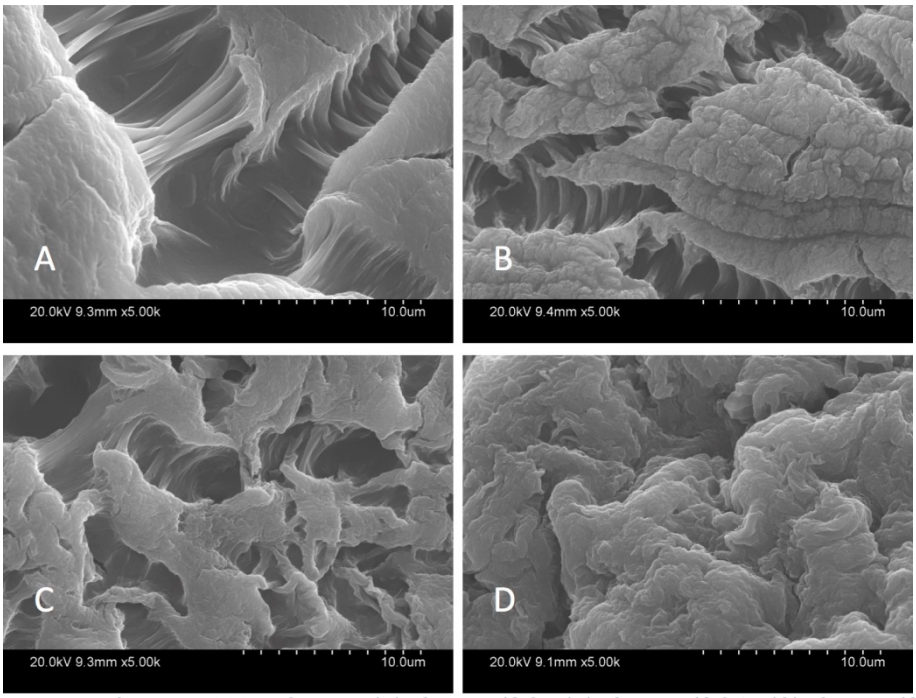

Figure 8 : SEM images, magnification 5000 x, Ca-Alg_2 (A), Ca-Alg_2/GO5 (B), Ca-Alg_2/GO10 (C), Ca-Alg_2/GO20 (D) beads

SEM images of dried beads show that an increase of concentration in graphene oxide, during the formulation of the beads, increases the porosity and the roughness of the beads. The morphological structure of Ca-Alg_2/GO20 is typically carbonaceous with similarities to activated carbon structure. With an increment in the porous nature of the beads, the surface available for the adsorption increases as well. Thus, there are more interactions between the adsorbate and the adsorbent, allowing a higher adsorption capacity of the pollutants on the surface of the beads [18].

3.2 Effect of the initial concentration

The effect of the initial concentration was studied using four different concentrations of MB, FMTD and DFC solution. The average of the results obtained for the adsorption of methylene blue at 10, 100, 500 and 1000 $mg \cdot L^{-1}$, famotidine at 10, 25, 100 and 250 $mg \cdot L^{-1}$ and diclofenac at 1, 5, 10 and 20 $mg \cdot L^{-1}$ are shown in Figure 9.

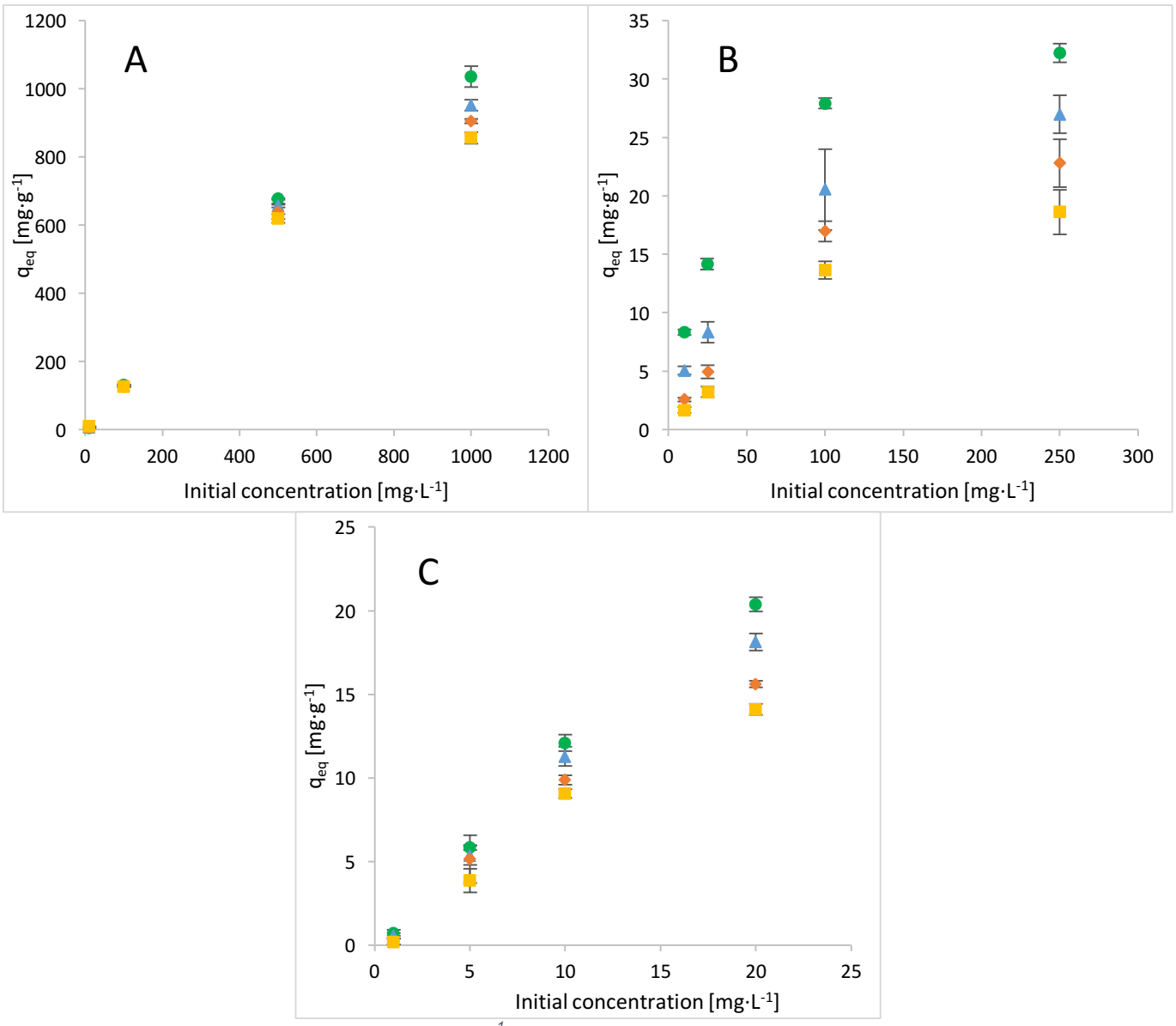

Figure 9 : Effect of the initial concentration on q_{eq} [$mg \cdot g^{-1}$] of methylene blue (A), famotidine (B) and diclofenac (C) using Ca-Alg_2 (■), Ca-Alg_2/GO5 (♦), Ca-Alg_2/GO10 (▲) and Ca-Alg_2/GO20 (●) dried beads. Average results are shown with standard deviation error bars (N=3).

The results show that when the initial concentration of the methylene blue, famotidine and diclofenac solution becomes higher, the adsorbed amount of drug at equilibrium q_{eq} ($mg \cdot g^{-1}$) increases as well. This is because that a bigger concentration increases the diffusion driving force of drug adsorbed by graphene oxide/alginate beads [44]. Therefore, it indicates that initial concentration plays an important role for MB, FMTD and DFC uptake. The results are significantly different between Ca-Alg_2 and Ca-Alg_2/GO20 beads showing that the increment of graphene oxide improves the adsorption capacity of the beads. This tendency can be observed for each pollutant and a gradient is also observed with beads at different concentration in graphene oxide. With an initial concentration of 1000 $mg \cdot L^{-1}$ for methylene blue, the obtained q_{eq} is 856 $\pm$ 17 $mg \cdot g^{-1}$ and 1036 $\pm$ 31 $mg \cdot g^{-1}$ for Ca-Alg_2 and Ca-Alg_2/GO20 beads respectively. Famotidine at an initial concentration of 250 $mg \cdot L^{-1}$ shows a q_{eq} of 18.6 $\pm$ 1.9 $mg \cdot g^{-1}$ and 32.2 $\pm$ 0.8 $mg \cdot g^{-1}$ for Ca-Alg_2 and Ca-Alg_2/GO20 beads respectively. Finally, for an initial concentration of 20 $mg \cdot L^{-1}$ of diclofenac, the q_{eq} obtained is 14.1 $\pm$ 0.3 $mg \cdot g^{-1}$ and 20.4 $\pm$ 0.4 $mg \cdot g^{-1}$ for Ca-Alg_2 and Ca-Alg_2/GO20 beads respectively.

3.3 Effect of the adsorbent dose

The effect of the adsorbent dose was studied by using four different concentrations of beads. The average of the results obtained for the adsorption of methylene blue, famotidine and diclofenac using 0.133, 0.333, 0.667 and 1.333 $g \cdot L^{-1}$ of Ca-Alg_2, Ca-Alg_2/GO5, Ca- Alg_2/GO10, Ca- Alg_2/GO20 dried beads are shown in Figure 10.

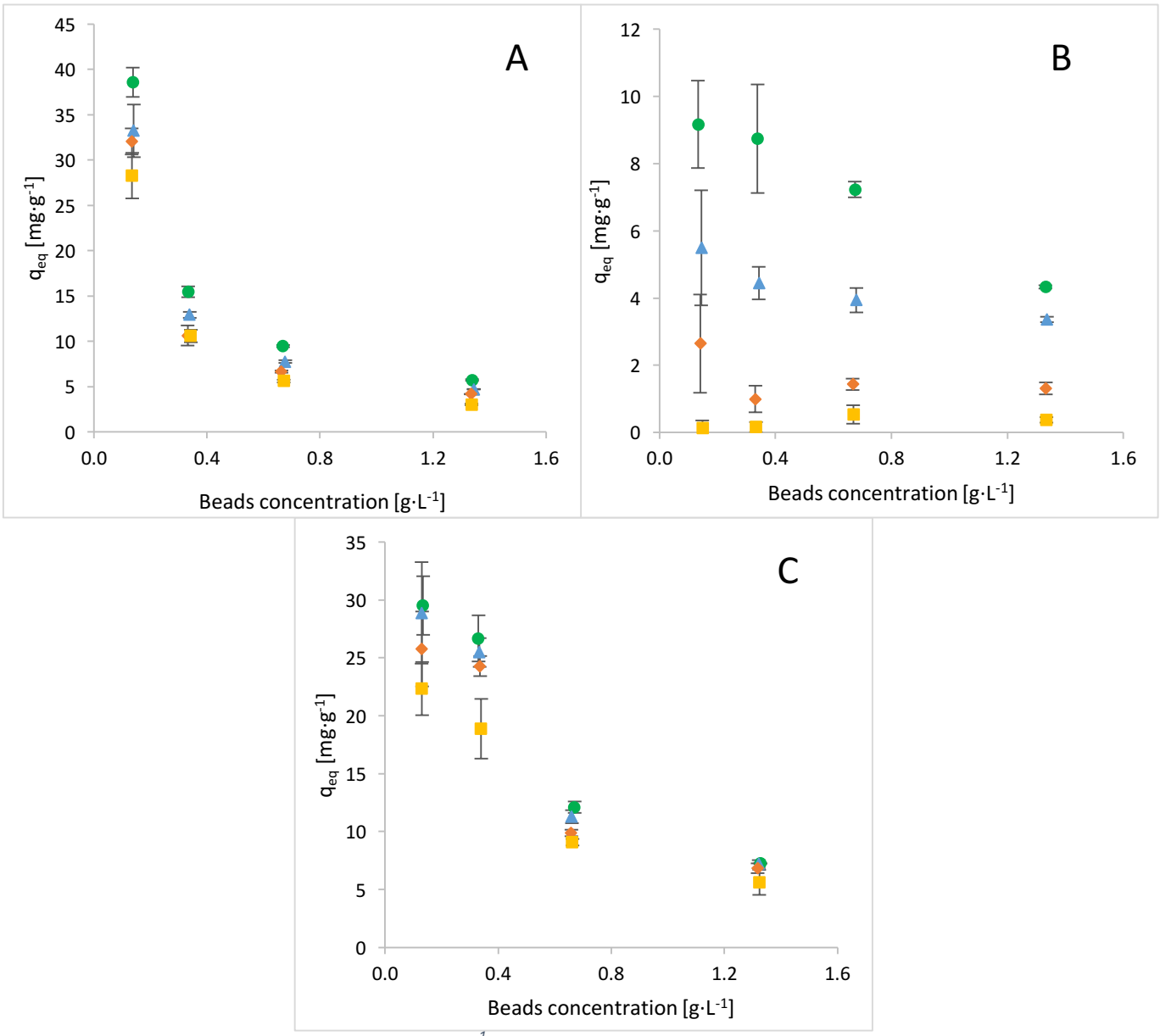

Figure 10 : Effect of the adsorbent dose on q_{eq} [mg·g^{-1}] of methylene blue (A), famotidine (B) and diclofenac (C) using Ca-Alg_2 (■), Ca-Alg_2/GO5 (♦), Ca-Alg_2/GO10 (▲) and Ca-Alg_2/GO20 (●) dried beads. Average results are shown with standard deviation error bars (N=3).

A decrease in the beads concentration leads to a significant increase of the adsorbed amount at equilibrium q_{eq} for the adsorption of methylene blue, famotidine and diclofenac. The adsorption capacity decreases with an increase of adsorbent due to a lower quantity adsorbed per unit weight of the adsorbent causing a decrease in the utility of active sites [45, 46]. The results show that Ca-Alg_2/GO20 beads present a better adsorption than Ca-Alg_2 beads. On the other hand, the removal percentage decreases also with a decrease in the beads concentration

because less sorption surface and less adsorption sites are available [47]. The highest q_{eq} observed is obtained with 0.133 $g \cdot L^{-1}$ of dried beads. For methylene blue, q_{eq} reaches 28.3 ± 2.5 $mg \cdot g^{-1}$ and 38.6 ± 1.6 $mg \cdot g^{-1}$ for Ca-Alg_2 and Ca-Alg_2/GO20 beads respectively. Adsorbed amount at equilibrium obtained with famotidine reaches 0.1 ± 0.2 $mg \cdot g^{-1}$ and 9.2 ± 1.3 $mg \cdot g^{-1}$ for Ca-Alg_2 and Ca-Alg_2/GO20 beads respectively. Finally, q_{eq} reaches 25.8 ± 3.2 $mg \cdot g^{-1}$ and 29.5 ± 2.5 $mg \cdot g^{-1}$ for Ca-Alg_2 and Ca-Alg_2/GO20 beads respectively with diclofenac.

3.4 Effect of the pH

The impact of the pH on adsorption was studied by using four different pH values. The average of the results obtained for the adsorption of methylene blue and famotidine at pH 7, 9, 10 and 11.5 and diclofenac at pH 2, 3.5, 5, 7 are shown in Figure 11.

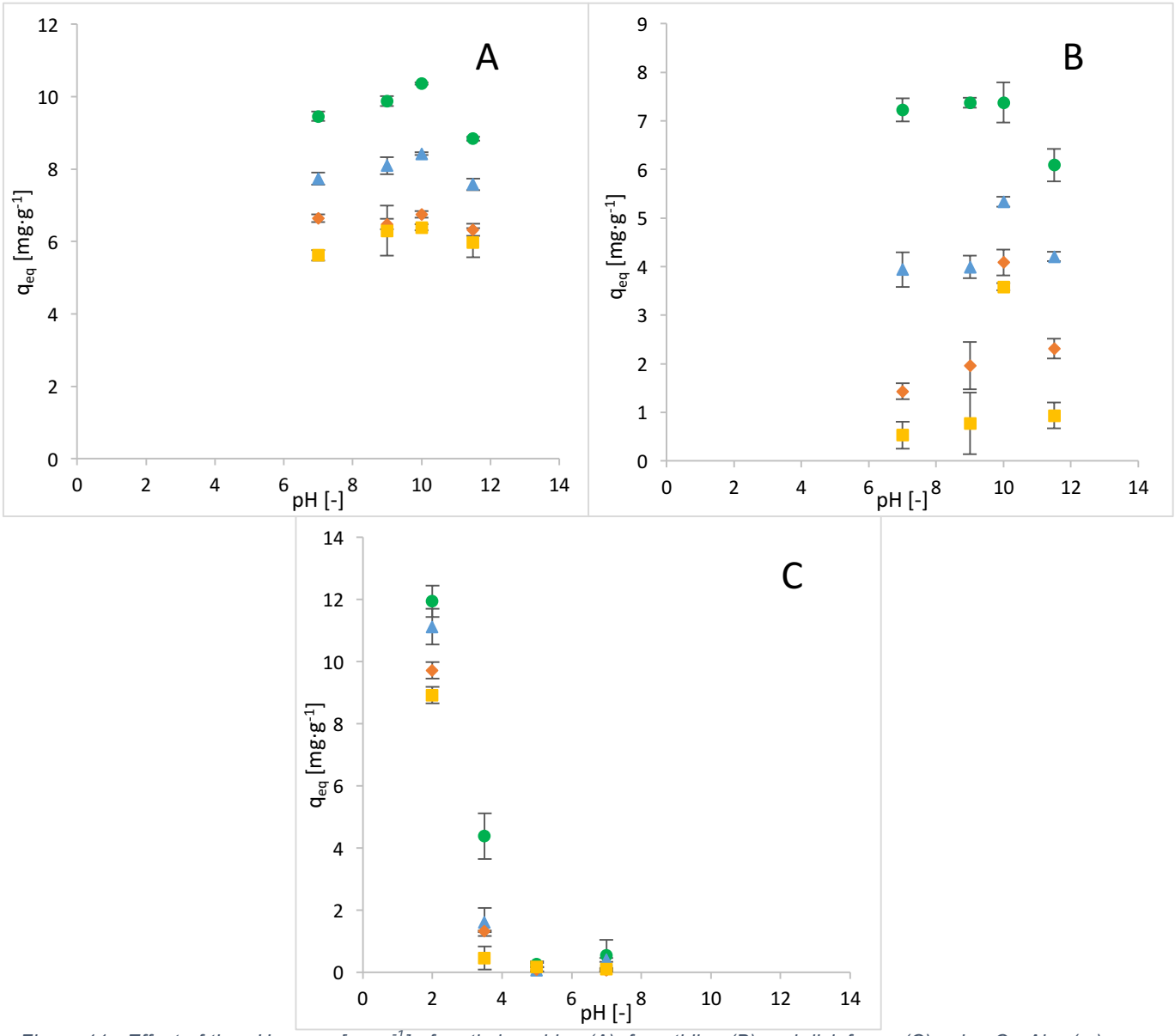

Figure 11 : Effect of the pH on q_{eq} [$mg \cdot g^{-1}$] of methylene blue (A), famotidine (B) and diclofenac (C) using Ca-Alg_2 (■), Ca-Alg_2/GO5 (♦), Ca-Alg_2/GO10 (▲) and Ca-Alg_2/GO20 (●) dried beads. Average results are shown with standard deviation error bars (N=3).

The highest q_{eq} obtained at pH 10 is 6.4 ± 0.1 $mg \cdot g^{-1}$ and 10.4 ± 0.0 $mg \cdot g^{-1}$ for methylene blue with Ca-Alg_2 and Ca-Alg_2/GO20 beads respectively. Adsorbed amount at equilibrium obtained with famotidine at pH 10 reaches 3.6 ± 0.1 $mg \cdot g^{-1}$ and 7.4 ± 0.4 $mg \cdot g^{-1}$ for Ca-Alg_2 and Ca-Alg_2/GO20 beads respectively. Finally, q_{eq} reaches 8.9 ± 0.3 $mg \cdot g^{-1}$ and 11.9 ± 0.5 $mg \cdot g^{-1}$ for Ca-Alg_2 and Ca-Alg_2/GO20 beads respectively with diclofenac at pH 2.

The results show that for cationic molecules, methylene blue and famotidine, the amount adsorbed at equilibrium increases slightly with a higher pH solution. It might due to more binding sites and functional groups, negatively charged, formed on the surface of graphene oxide beads which increases the surface complexion capacity and ion exchange [48]. Indeed, the oxygen functional groups in the structure of the Ca-Alg_2 and Ca-Alg_2/GO beads are dissociated at high pH values, making the adsorbent negatively charged [49]. As the pH decreases, the adsorption process becomes lower due to the protons competition with the cationic molecules for the available adsorption sites [50]. However, beads may be negatively affected or damaged at pH 11.5 because q_{eq} drops at pH 11.5. On the other hand, the results for the anionic molecule, diclofenac, show than the adsorbed amount at equilibrium is significantly enhanced at low pH. At acidic pH value, diclofenac has neutral ion species which promotes the attraction to Ca-Alg_2 and graphene oxide [51], with similar behaviour also previously reported [52]. As observed, the initial pH of the solution affects the surface charge of the adsorbent and the ionization behaviour of the adsorbate and adsorbent [22].

3.5 Effect of the temperature

Adsorption studies were performed across three temperatures ranging from 4 to 30 degrees Celcius. The average of the results obtained for the adsorption of methylene blue, famotidine and diclofenac at 4, 22 (room temperature) and 30 degrees Celsius are shown in Figure 12 below.

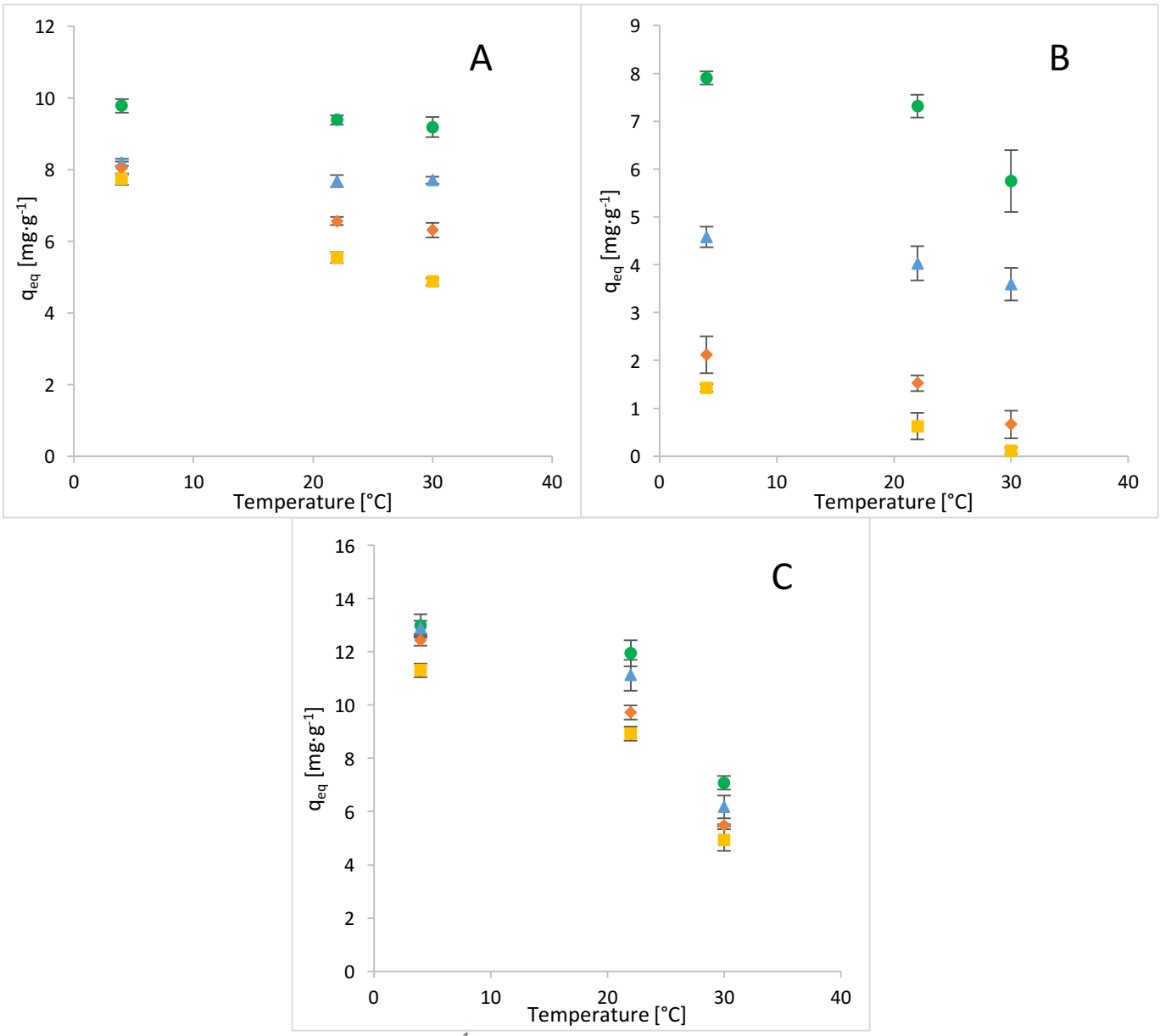

Figure 12 : Effect of the temperature on q_{eq} [mg·g^{-1}] of methylene blue (A), famotidine (B) and diclofenac (C) using Ca-Alg$_2$ (■), Ca-Alg$_2$/GO5 (♦), Ca-Alg$_2$/GO10 (▲) and Ca-Alg$_2$/GO20 (●) dried beads. Average results are shown with standard deviation error bars (N=3).

The coldest temperature, 4°C, shows a better amount adsorbed at equilibrium for each pollutant. The adsorption process decreases with an increase in temperature. For methylene blue at 4°C, q_{eq} obtained is 7.7 ± 0.2 mg·g^{-1} and 9.8 ± 0.2 mg·g^{-1} with Ca-Alg$_2$ and Ca-Alg$_2$/GO20 beads respectively. Adsorbed amount at equilibrium obtained with famotidine at 4°C reaches 1.4 ± 0.1 mg·g^{-1} and 7.9 ± 0.1 mg·g^{-1} for Ca-Alg$_2$ and Ca-Alg$_2$/GO20 beads respectively. Finally, q_{eq} reaches 11.3 ± 0.3 mg·g^{-1}

and 13.0 ± 0.4 $mg \cdot g^{-1}$ for Ca-Alg_2 and Ca-Alg_2/GO20 beads respectively with diclofenac at 4°C. The decrease in adsorption capacity with an increase in temperature can be explained by an exothermic adsorption process (see section 3.6) [53].

3.6 Thermodynamics studies

The thermodynamics studies were conducted based on the feasibility and the spontaneous nature of the adsorption. Distribution coefficient for the adsorption K_d , enthalpy change ΔH°, entropy change ΔS° and Gibbs free energy change ΔG° were calculated using Equations 2, 3 and 4 reported in the method section. The results obtained are shown in the Tables 2, 3 and 4 below.

Table 2 : Thermodynamic parameters for MB adsorption on Ca-Alg_2, Ca-Alg_2/GO5, Ca-Alg_2/GO10 and Ca-Alg_2/GO20 beads

Adsorbent	K_d [-]			ΔG° [kJ·mol^{-1}]			ΔH° [kJ·mol^{-1}]	ΔS° [J·K^{-1}·mol^{-1}]
	277K	295K	303K	277K	295K	303K		
Ca-Alg_2	1.07	0.59	0.48	-0.144	1.240	1.855	-21.44	-76.9
Ca-Alg_2/GO5	1.18	0.77	0.73	-0.341	0.504	0.879	-13.34	-46.9
Ca-Alg_2/GO10	1.19	1.08	1.04	-0.401	-0.186	0.091	-3.712	-12.0
Ca-Alg_2/GO20	1.88	1.68	1.60	-1.459	-1.272	-1.189	-4.338	-10.4

Table 3 : Thermodynamic parameters for FMTD adsorption on Ca-Alg_2, Ca-Alg_2/GO5, Ca-Alg_2/GO10 and Ca-Alg_2/GO20 beads

Adsorbent	K_d [-]			ΔG° [kJ·mol^{-1}]			ΔH° [kJ·mol^{-1}]	ΔS° [J·K^{-1}·mol^{-1}]
	277K	295K	303K	277K	295K	303K		
Ca-Alg_2	0.11	0.04	0.01	4.747	9.465	11.56	-67.85	-262
Ca-Alg_2/GO5	0.17	0.11	0.05	3.926	6.226	7.248	-31.46	-128
Ca-Alg_2/GO10	0.44	0.38	0.32	1.847	2.505	2.797	-8.277	-36.6
Ca-Alg_2/GO20	1.14	0.98	0.63	-0.418	0.473	0.868	-14.13	-49.5

Table 4 : Thermodynamic parameters for DFC adsorption on Ca-Alg2, Ca-Alg2/GO5, Ca-Alg2/GO10 and Ca-Alg2/GO20 beads

Adsorbent	K_d [-]			ΔG° [kJ·mol^{-1}]			ΔH° [kJ·mol^{-1}]	ΔS° [J·K^{-1}·mol^{-1}]
	277 K	295K	303K	277K	295K	303K		
Ca-Alg_2	2.90	1.55	0.55	-2.758	-0.042	1.165	-44.56	-151
Ca-Alg_2/GO5	4.96	1.80	0.58	-3.982	-0.704	0.753	-54.43	-182
Ca-Alg_2/GO10	5.48	2.61	0.74	-4.352	-1.342	-0.004	-50.67	-167
Ca-Alg_2/GO20	6.88	3.81	0.93	-4.896	-2.047	-0.781	-48.74	-158

The capability of the Ca-Alg_2 and Ca-Alg_2/GO beads to adsorb a solute is demonstrated by the distribution coefficient K_d and it also shows the extent of its movement in a solution phase [54]. The K_d values can be compared between the adsorption capacities of different adsorbents when performed under the same experimental conditions which makes it a useful parameter [55]. As the results show, the K_d values are higher for a lower temperature and for the Ca-Alg_2/GO20 beads indicating a better adsorption. Furthermore, the negative values of the enthalpy change ΔH° show that the adsorption process is exothermic meaning that the

adsorption increases with a decrease in temperature [56]. The negative values of the entropy change $\Delta S°$ mean a decrease of randomness at the solid-solute interface. Moreover, a negative value of Gibbs free energy change $\Delta G°$ means that the adsorption process is spontaneous. Several studies indicate that the absolute magnitude of the change in free energy for physisorption is between −20 kJ·mol^{-1} and 0 kJ·mol^{-1} and that chemisorption occurs between −80 kJ·mol^{-1} and −400 kJ·mol^{-1} [57, 58, 59]. Thus, adsorption process observed seems to be physisorption.

3.7 Effect of the contact time

The effect of the contact time on q_t was studied by taking samples over 24 hours. The average of the results obtained for the adsorption of methylene blue, famotidine and diclofenac are shown in Figure 13 below.

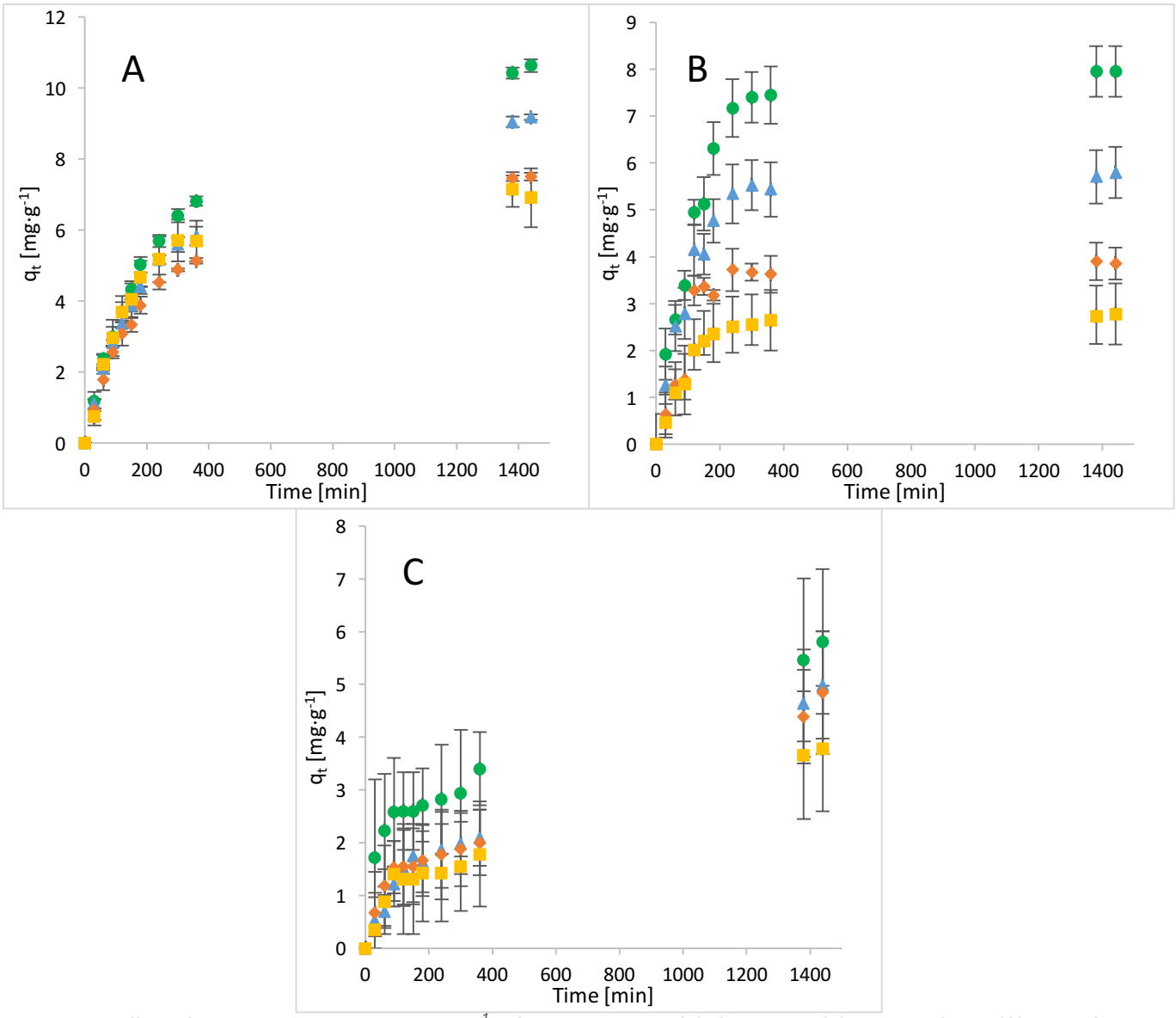

Figure 13 : Effect of the contact time on q_{eq} [mg·g^{-1}] of methylene blue (A), famotidine (B) and diclofenac (C) using Ca-Alg$_2$ (■), Ca-Alg$_2$/GO5 (♦), Ca-Alg$_2$/GO10 (▲) and Ca-Alg$_2$/GO20 (●) dried beads. Average results are shown with standard deviation error bars (N=3).

After 24 hours of contact time, the results show that the adsorption process reaches equilibrium. The adsorption gradually increases with the contact time and slows down progressively to reach a plateau. Ca-Alg_2/GO20 beads are the most efficient for the adsorption of each compound as expected. The amount adsorbed of MB at equilibrium obtained is 6.9 $\pm$ 0.8 $mg \cdot g^{-1}$ and 10.6 $\pm$ 0.2 $mg \cdot g^{-1}$ for Ca-Alg_2 and Ca-Alg_2/GO20 beads respectively. With famotidine, q_{eq} reaches 2.8 $\pm$ 0.7 $mg \cdot g^{-1}$ and 8.0 $\pm$ 0.5 $mg \cdot g^{-1}$ for Ca-Alg_2 and Ca-Alg_2/GO20 beads respectively. Finally, q_{eq} observed for diclofenac is 3.8 $\pm$ 1.2 $mg \cdot g^{-1}$ and 5.8 $\pm$ 1.4 $mg \cdot g^{-1}$ for Ca-Alg_2 and Ca-Alg_2/GO20 beads respectively.

3.8 Kinetics

Three models were fitted to the experimental data. Pseudo-first-order Lagergren, pseudo-second model and intraparticle diffusion model are shown in Figure 14 below.

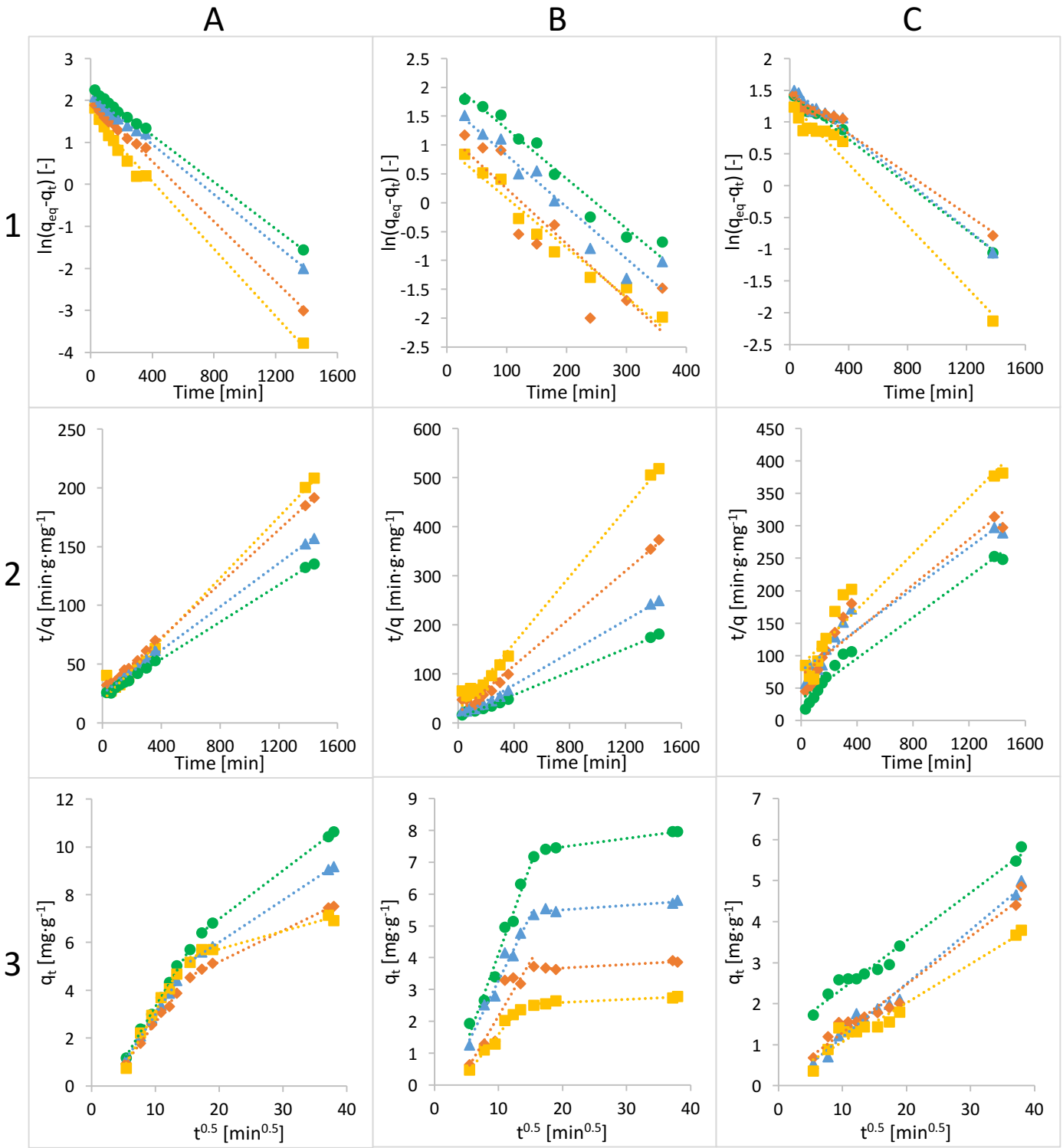

Figure 14 : Linearized-integral form of the pseudo-first-order Lagergren equation of methylene blue (A1), famotidine (B1) and diclofenac (C1), linearized-integral form of the pseudo-second-order model of methylene blue (A2), famotidine (B2) and diclofenac (C2) and intraparticle diffusion model of methylene blue (A3), famotidine (B3) and diclofenac (C3) using Ca-Alg$_2$ (■), Ca-Alg$_2$/GO5 (♦), Ca-Alg$_2$/GO10 (▲) and Ca-Alg$_2$/GO20 (●) dried beads.

All of the kinetic parameters calculated for the adsorption of MB, FMTD and DFC are shown in Tables 5, 6 and 7 below.

Table 5: Kinetic parameters for MB adsorption onto Ca-Alg$_2$, Ca-Alg$_2$/GO5, Ca-Alg$_2$/GO10 and Ca-Alg$_2$/GO20 dried beads.

Adsorbent	Pseudo-first order			Pseudo-second order			Intraparticle diffusion					
	q_{eq} [mg·g^{-1}]	k_1 [min^{-1}]	R^2 [-]	q_{eq} [mg·g^{-1}]	k_2 [g·mg^{-1}·min^{-1}]	R^2 [-]	$k_{id,1}$ [mg·g^{-1}·min$^{-0.5}$]	C_1 [mg·g^{-1}]	R^2 [-]	$k_{id,2}$ [mg·g^{-1}·min$^{-0.5}$]	C_2 [mg·g^{-1}]	R^2 [-]
Ca-Alg$_2$	6.27	$5.1\cdot10^{-3}$	0.9657	7.84	$8.3\cdot10^{-4}$	0.9907	0.479	-1.68	0.9875	0.0749	4.22	0.9580
Ca-Alg$_2$/GO5	7.22	$3.6\cdot10^{-3}$	0.9974	8.70	$5.0\cdot10^{-4}$	0.9995	0.358	-0.957	0.9950	0.128	2.69	0.9997
Ca-Alg$_2$/GO10	8.55	$3.0\cdot10^{-3}$	0.9979	10.81	$3.5\cdot10^{-4}$	0.9991	0.409	-1.10	0.9993	0.178	2.47	0.9996
Ca-Alg$_2$/GO20	9.79	$2.8\cdot10^{-3}$	0.9991	12.66	$2.7\cdot10^{-4}$	0.9993	0.457	-1.28	0.9958	0.202	2.94	0.9998

Table 6 : Kinetic parameters for FMTD adsorption onto Ca-Alg$_2$, Ca-Alg$_2$/GO5, Ca-Alg$_2$/GO10 and Ca-Alg$_2$/GO20 dried beads.

Adsorbent	Pseudo-first order			Pseudo-second order			Intraparticle diffusion					
	q_{eq} [mg·g^{-1}]	k_1 [min^{-1}]	R^2 [-]	q_{eq} [mg·g^{-1}]	k_2 [g·mg^{-1}·min^{-1}]	R^2 [-]	$k_{id,1}$ [mg·g^{-1}·min$^{-0.5}$]	C_1 [mg·g^{-1}]	R^2 [-]	$k_{id,2}$ [mg·g^{-1}·min$^{-0.5}$]	C_2 [mg·g^{-1}]	R^2 [-]
Ca-Alg$_2$	2.57	$8.6\cdot10^{-3}$	0.9597	2.93	$4.6\cdot10^{-3}$	0.9940	0.248	-0.882	0.9699	0.0098	2.39	0.8809
Ca-Alg$_2$/GO5	3.32	$9.5\cdot10^{-3}$	0.7828	4.15	$2.9\cdot10^{-3}$	0.9881	0.340	-1.23	0.8596	0.0116	3.44	0.9355
Ca-Alg$_2$/GO10	5.57	$9.0\cdot10^{-3}$	0.9315	6.06	$2.5\cdot10^{-3}$	0.9969	0.409	-0.821	0.9656	0.0137	5.23	0.8817
Ca-Alg$_2$/GO20	8.50	$8.6\cdot10^{-3}$	0.9631	8.50	$1.4\cdot10^{-3}$	0.9960	0.556	-1.44	0.9742	0.0271	6.93	0.9992

Table 7 : Kinetic parameters for DFC adsorption onto Ca-Alg2, Ca-Alg2/GO5, Ca-Alg2/GO10 and Ca-Alg2/GO20 dried beads.

Adsorbent	Pseudo-first order			Pseudo-second order			Intraparticle diffusion		
	q_{eq} [mg·g^{-1}]	k_1 [min^{-1}]	R^2 [-]	q_{eq} [mg·g^{-1}]	k_2 [g·mg^{-1}·min^{-1}]	R^2 [-]	k_{id} [mg·g^{-1}·min$^{-0.5}$]	C [mg·g^{-1}]	R^2 [-]
Ca-Alg$_2$	3.70	$2.4\cdot10^{-3}$	0.9756	4.64	$5.5\cdot10^{-4}$	0.9405	0.095	0.107	0.9684
Ca-Alg$_2$/GO5	4.28	$1.6\cdot10^{-3}$	0.9820	5.72	$4.4\cdot10^{-4}$	0.9147	0.117	0.110	0.9740
Ca-Alg$_2$/GO10	4.74	$1.9\cdot10^{-3}$	0.9865	6.31	$3.3\cdot10^{-4}$	0.9422	0.131	-0.130	0.9858
Ca-Alg$_2$/GO20	4.26	$1.8\cdot10^{-3}$	0.9879	6.33	$7.7\cdot10^{-4}$	0.9712	0.117	1.190	0.9835

The adsorbed amount of methylene blue and famotidine predicted using the pseudo-first-order model are lower than the experimental data. Furthermore, the values of correlation coefficient R^2 are better for the pseudo-second-order. This indicates that the adsorption process does not fit the pseudo-first-order and shows the applicability to the pseudo-second-order to describe the adsorption of methylene blue and famotidine onto Ca-Alg_2 and Ca-Alg_2/GO beads [60].

The diffusion mechanism during the adsorption process was studied by the intraparticle diffusion model. The plot of q_t versus $t^{1/2}$ shows a non-linear form indicating that the adsorption process occurs in more than one step as there is two distinct linear regions. The first straight region is attributed to the macro-pore diffusion and the second linear region to micro-pore diffusion. The first portion characterizes the instantaneous utilization of the adsorbing sites on the adsorbent surface. On the other hand, the second region is attributed to a slow diffusion of the methylene blue from the surface film into the micro-pores [61]. These micro-pores are the least accessible sites of adsorption. Indeed, this also stimulates a very slow rate of migration of adsorbates from the liquid phase on to the adsorbent surface. A deviation in the straight line from the origin might be due to the difference in rate of mass transfer in the initial and final stages of adsorption [62]. Further deviation of straight lines from the origin indicates that the pore diffusion is not the only rate-limiting step in the adsorption process [63]. The values of the intercept are linked to the thickness of the boundary layer meaning that the larger the intercept is the greater is the boundary layer effect [64].

The predictions for the adsorbed amount of diclofenac obtained using the pseudo-first-order model fit the experimental data better than those obtained using the pseudo-second-order model. Moreover, the values of correlation coefficient R^2 are higher for the pseudo-first-order model meaning that the adsorption process of diclofenac onto Ca-Alg_2 and Ca-Alg_2/GO beads can be described by the Lagergren model. The intraparticle diffusion model shows a straight line indicating the adsorption mechanism follows the intraparticle diffusion process only because the intercept is close to 0 [65]. However, with Ca-Alg_2/GO20 the boundary layer is thicker indicating that the boundary layer effect might influence also the rate of diffusion.

3.9 Adsorption isotherms

The adsorption isotherms for methylene blue were built by testing nine different concentrations namely 1, 5, 10, 25, 50, 100, 250, 500 and 1000 $mg \cdot L^{-1}$. The adsorption was carried out over 24 hours at 125 rpm, room temperature and pH 7 with 0.05 g of beads. The isotherms obtained for each kind of beads are shown in Figure 15 below.

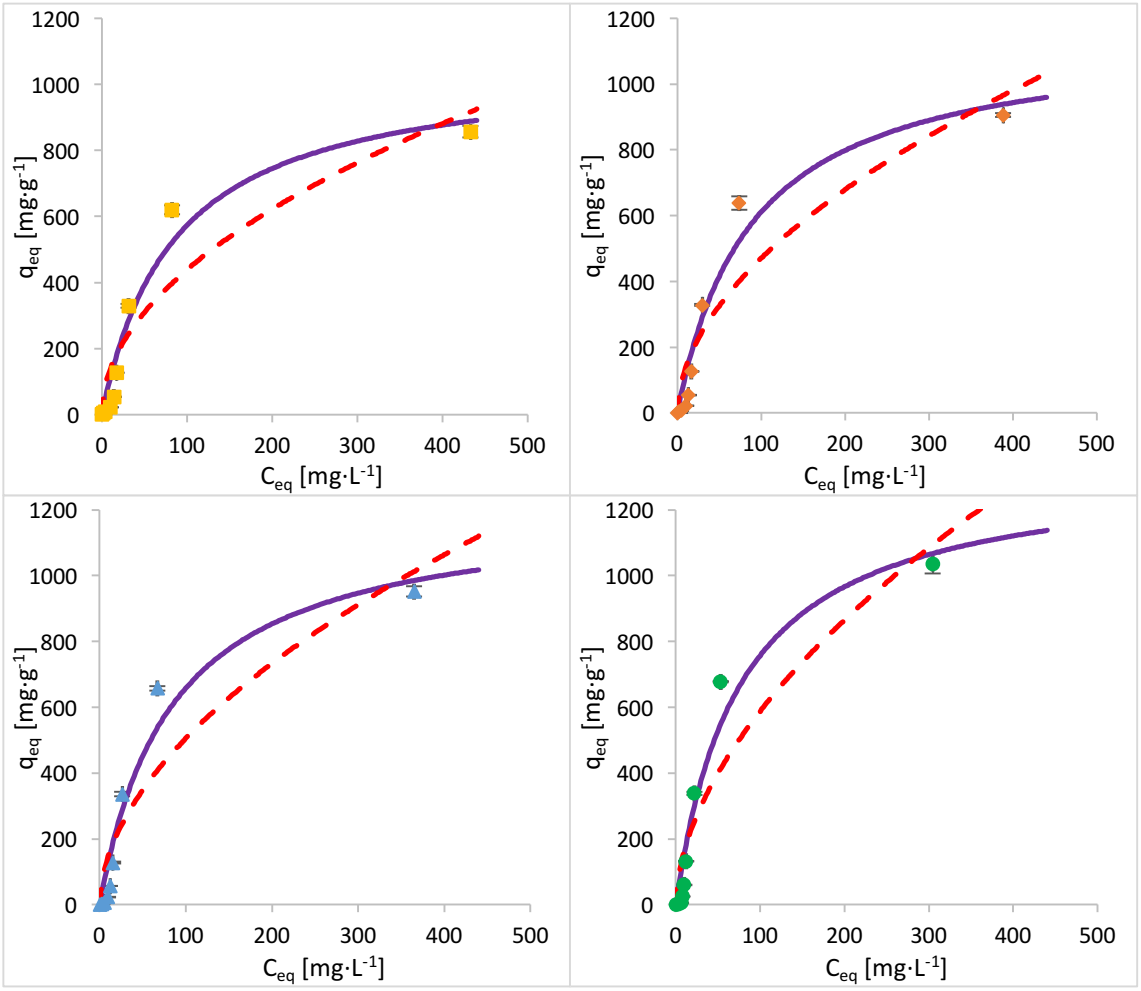

Figure 15 : Adsorption isotherms for methylene blue using Ca-Alg$_2$ (■), Ca-Alg$_2$/GO5 (♦), Ca-Alg$_2$/GO10 (▲) and Ca-Alg$_2$/GO20 (●) dried beads with Langmuir (-) and Freundlich (--) models. Average results are shown with standard deviation error bars (N=3).

The results obtained show that an increase in graphene oxide concentration during the making of the beads improves the adsorbed amount of dye at equilibrium. The Langmuir model fits the experimental data better than the Freundlich model as indicated by goodness-of-fit tests (see Tables 8, 9 and 10).

The adsorption isotherms for famotidine were performed by using 1, 5, 10, 25, 50, 100 and 250 $mg \cdot L^{-1}$ of solution whereas for diclofenac the concentrations were 1, 5, 10, 15 and 20 $mg \cdot L^{-1}$. The adsorption process was carried out over 24 hours at 125 rpm, room temperature and pH 7 with 0.05 g of beads. The results are shown in Figure 16 and 17 below.

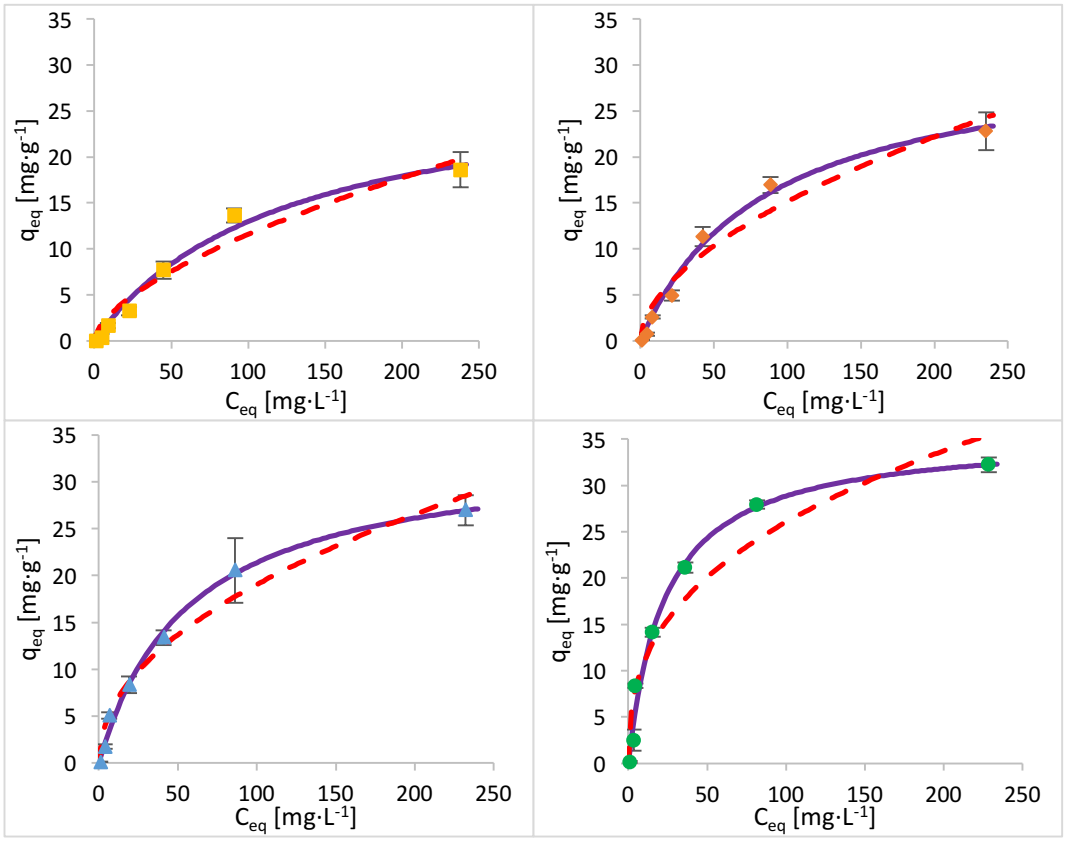

Figure 16 : Adsorption isotherms of famotidine using Ca-Alg2 (■), Ca-Alg$_2$/GO5 (♦), Ca-Alg$_2$/GO10 (▲) and Ca-Alg$_2$/GO20 (●) dried beads with Langmuir (-) and Freundlich (--) models. Average results are shown with standard deviation error bars (N=3).

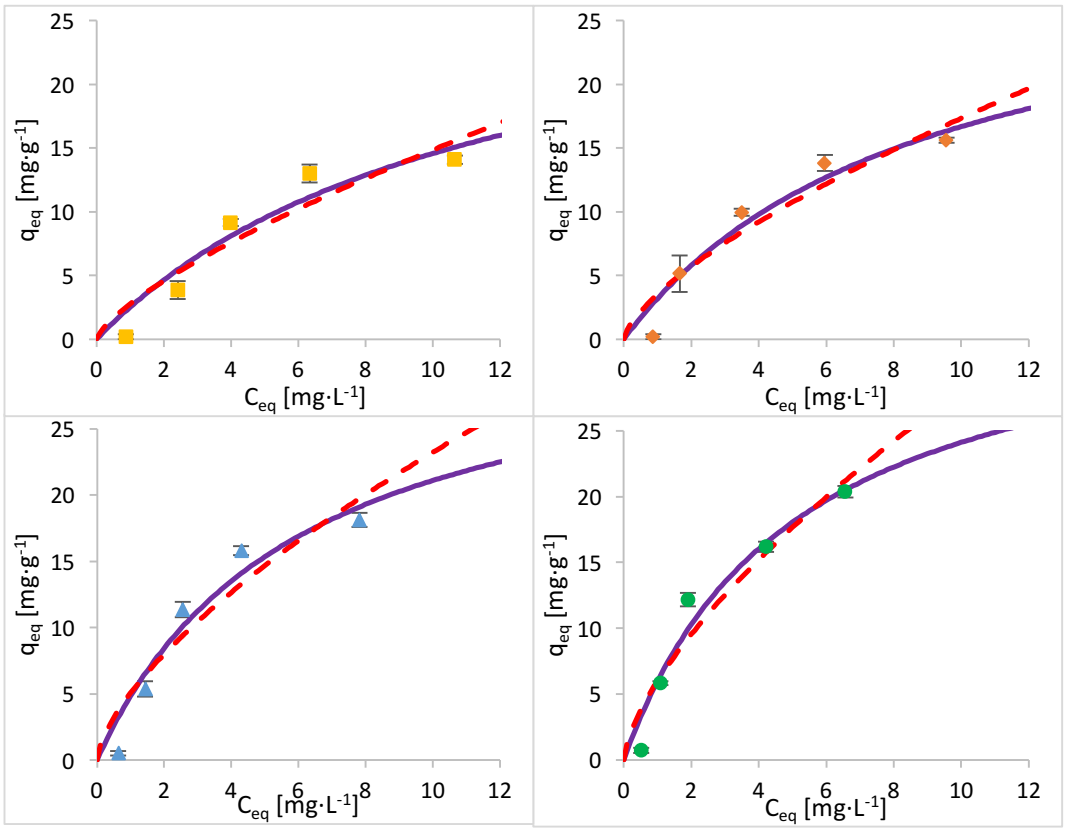

Figure 17 : Adsorption isotherms of diclofenac using Ca-Alg2 (■), Ca-Alg$_2$/GO5 (♦), Ca-Alg$_2$/GO10 (▲) and Ca-Alg$_2$/GO20 (●) dried beads with Langmuir (-) and Freundlich (--) models. Average results are shown with standard deviation error bars (N=3).

The results for the adsorption isotherms of famotidine and diclofenac indicate similar behaviours than for methylene blue. Indeed, the Langmuir model fits better the experimental data for each compound with every different kind of beads.
Tables 8, 9 and 10 below present the Langmuir and Freundlich isotherm constants and correlation coefficients for the methylene blue, famotidine and diclofenac adsorption.

Table 8 : Langmuir and Freundlich isotherm constants for MB adsorption onto Ca-Alg$_2$ and Ca-Alg$_2$/GO beads

Adsorbent	Langmuir			Freundlich		
	q_{max} [mg·g^{-1}]	K_L [L·g^{-1}]	R^2 [-]	K_F [L·g^{-1}]	n [-]	R^2 [-]
Ca-Alg$_2$	1064	85.56	0.9778	43.26	0.503	0.9270
Ca-Alg$_2$/GO5	1153	88.93	0.9716	41.02	0.530	0.9109
Ca-Alg$_2$/GO10	1212	84.21	0.9782	42.64	0.537	0.8941
Ca-Alg$_2$/GO20	1334	76.21	0.9894	45.10	0.558	0.8541

Table 9 : Langmuir and Freundlich isotherm constants for FMTD adsorption onto Ca-Alg$_2$ and Ca-Alg$_2$/GO beads

Adsorbent	Langmuir			Freundlich		
	q_{max} [mg·g^{-1}]	K_L [L·g^{-1}]	R^2 [-]	K_F [L·g^{-1}]	n [-]	R^2 [-]
Ca-Alg$_2$	28.96	123.2	0.9809	0.680	0.615	0.9351
Ca-Alg$_2$/GO5	31.69	85.39	0.9733	1.190	0.552	0.9173
Ca-Alg$_2$/GO10	33.57	57.02	0.9611	2.099	0.479	0.8593
Ca-Alg$_2$/GO20	35.50	23.10	0.9214	4.647	0.374	0.7491

Table 10 : Langmuir and Freundlich isotherm constants for DFC adsorption onto Ca-Alg$_2$ and Ca-Alg$_2$/GO beads

Adsorbent	Langmuir			Freundlich		
	q_{max} [mg·g^{-1}]	K_L [L·g^{-1}]	R^2 [-]	K_F [L·g^{-1}]	n [-]	R^2 [-]
Ca-Alg$_2$	30.74	11.10	0.9457	2.795	0.725	0.8937
Ca-Alg$_2$/GO5	31.81	9.020	0.9175	3.441	0.705	0.8707
Ca-Alg$_2$/GO10	33.72	5.988	0.8886	5.055	0.662	0.8401
Ca-Alg$_2$/GO20	36.35	5.066	0.8872	5.992	0.672	0.8322

The values of R^2 are higher with Langmuir model indicating that this model fits better the experimental data than the Freundlich isotherm for each kind of beads and each pharmaceutical. The Langmuir model supposes that the adsorption process occurs on a homogenous surface by monolayer adsorption.
Constants K_F and n indicate the adsorption capacity and the adsorption intensity respectively. As indicated by the experimental data, the adsorption capacity K_F is increasing gradually with graphene oxide concentration and constant n is lower than 1 meaning the adsorption isotherm is favourable. Maximum adsorption capacities q_{max} obtained are 1334, 35,50 and 36.35 mg·g^{-1} for the uptake of methylene blue, famotidine and diclofenac respectively. It means that Ca-Alg$_2$/GO beads are an efficient adsorbent for the removal of these pharmaceuticals, particularly for methylene blue as, to our knowledge, this is the highest adsorption capacity for MB

that been reported in the literature. Table 11 below presents the maximum adsorption capacity for the uptake of methylene blue reported in several studies.

Table 11 : Adsorption capacity for the adsorption of methylene blue reported in the literature

Adsorbent	Adsorption capacity [$mg \cdot g^{-1}$]	Reference
Activated carbon (coconut shells)	1030.0	20
Commercial activated carbon	980.3	64
Teak wood bark	914.59	67
Ca-Alg_2/activated carbon composites	892.0	23
Poly(methacrylic acid) modified biomass	869.6	68
Ca-Alg_2 beads	800.0	20
graphene oxide	714.0	66
Poly(amic acid) modified biomass of baker's yeast	680.3	69
Activated carbon produced from New Zealand coal	588	70
Papaya seeds	555.55	45
Polyvilnyldienefluoride activated carbon fibers	486	71
Filtrasorb 400	476	70
Straw activated carbon	472.10	64
Grass waste	457.64	72
Bamboo based activated carbon	454.20	73
Activated carbon (molasses/sulphuric acid)	435	74
Activated carbon prepared from coconut husk	434.78	75
Vetiver roots activated carbon-H_20	423	76
Caulerpa lentillifera	417	77
Peach stones based activated carbon	412	78
Activated carbon	400	79
Oil palm fiber-based activated carbon	400	80
Pomelo (*Citrus grandis*) peel	344.83	81
Rice husk activated carbon	343.50	64
Peat	324	82
Coal	323.68	67
Clay	300	83
Montmorillonite clay	289.12	84
Alga *Sargassum muticum* seaweed	279.2	85
coconut shell activated carbon	277.90	64
***Enteromorpha* spp.**	274	86
Diatomite	198	87
Perlite	162.3	88
pH activated, dried Ca-Alg_2	1064	This study
pH activated, dried Ca-Alg_2/GO5	1153	This study
pH activated, dried Ca-Alg_2/GO10	1212	This study
pH activated, dried Ca-Alg_2/GO20	1334	This study

Table 12 below presents the maximum adsorption capacity for the uptake of famotidine reported in several studies.

Table 12 : Adsorption capacity on the adsorption of famotidine reported in the literature

Adsorbent	Adsorption capacity [$mg \cdot g^{-1}$]	Reference
bifunctionalized mesoporous silica COOH/SBA-15	396.9	96
carboxylic-modified mesoporous silica MSU-3	342.54	95
carboxylic-modified mesoporous silica MSU-2	307.92	95
carboxylic acid functionalized SBA-15 materials	203.95	93
carboxylic-modified mesoporous silica MSU-1	155.52	95
Grafted nano-polymer	116.3	94
Activated carbon	86.20	89
pH activated, dried Ca-Alg_2	28.96	This study
pH activated, dried Ca-Alg_2/GO5	31.69	This study
pH activated, dried Ca-Alg_2/GO10	33.57	This study
pH activated, dried Ca-Alg_2/GO20	35.50	This study

Table 13 below presents the maximum adsorption capacity for the uptake of diclofenac reported in several studies.

Table 13 : Adsorption capacity on the adsorption of diclofenac reported in the literature

Adsorbent	Adsorption capacity [$mg \cdot g^{-1}$]	Reference
Graphene oxide	500	52
Oxidized activated carbon	487	101
Expanded graphite	330	98
Metal-organic frameworks	263	99
Activated carbon from *Terminalia catappa*	91	104
Grape bagasse	77	102
Commercial activated carbon	76	99
Organoclay BDTA-Mt	63.4	97
Activated carbon from cocoa shell	63	103
Organoclay HDTMA-Mt	57.7	97
Activated carbon from olive-waste cakes	56.2	90
Carbon nanotubes/alumina	27	105
Modified multi-walled carbon nanotubes	23.1	91
***Cyclamen persicum* tubers based activated carbon**	22.22	92
Olive stones activated carbon	11.0	100
pH activated, dried Ca-Alg_2	31.23	This study
pH activated, dried Ca-Alg_2/GO5	31.44	This study
pH activated, dried Ca-Alg_2/GO10	33.72	This study
pH activated, dried Ca-Alg_2/GO20	36.35	This study

3.10 Desorption

The desorption of each compound adsorbed onto Ca-Alg_2 and Ca-Alg_2/GO beads was studied by using HCl/NaOH 0.1M, NaCl 1M and ethanol 1% v:v. The results of the percentage desorbed after 24 hours are shown in Figure 18 below.

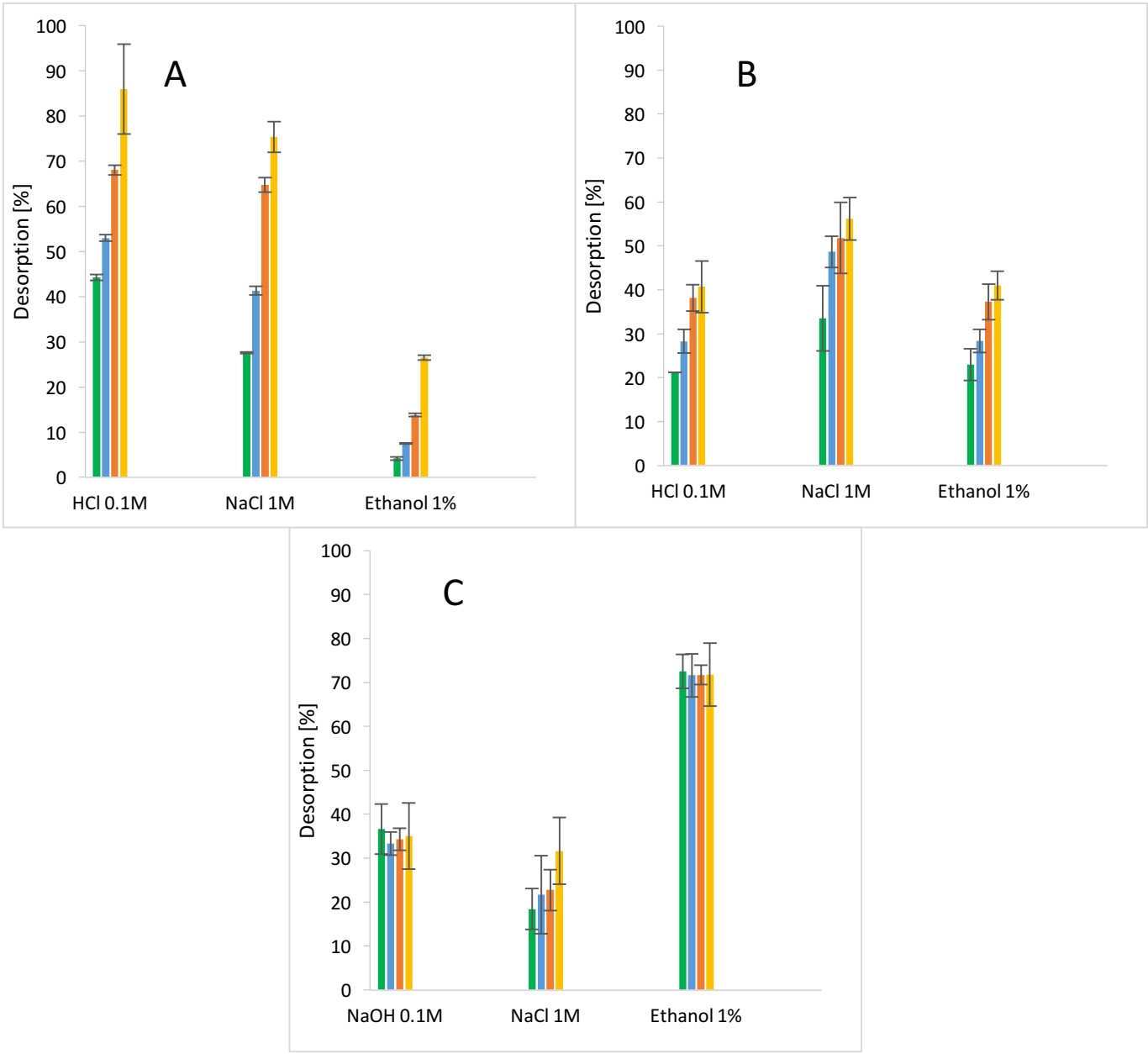

Figure 18 : Desorption [%] of methylene blue (A), famotidine (B) and diclofenac (C) with Ca-Alg2 (■), Ca-Alg_2/GO5 (■), Ca-Alg_2/GO10 (■) and Ca-Alg_2/GO20 (■) dried beads using HCl or NaOH 0.1M, NaCl 1M and ethanol 1%. Average results are shown with standard deviation error bars (N=3).

The desorption of methylene blue from the beads is higher when using HCl 0.1 M than with NaCl or ethanol. The results show that 89 ± 9.9 % and 44 ± 0.6 % of MB are desorbed for Ca-Alg_2 and Ca-Alg_2/GO20 beads respectively. Indeed, protons H^+ in excess seem able to force the cationic dye to be released by taking place on the adsorption sites on the surface of the beads. It is more difficult to effect release of methylene blue from beads with graphene oxide due to a stronger affinity. NaCl 1 M shows also good results for the desorption of MB. However, the ionic strength of

sodium chloride 1 M destabilizes the structure of calcium alginate beads, making them soft, fragile and crumbly. As such, high concentration salt solution cannot be use as a desorbent due to the inability to reuse the beads. Ethanol solution shows little desorption of MB as the main interactions between adsorbate and adsorbent are typically ionic bonds and ethanol has little effect to remove the dye from the beads with van der Waals' forces.

On the other hand, the desorption of famotidine using HCl 0.1 M shows less satisfactory results. It might be due to a poor solubility at low pH solution or due to hydrogen bonds between the adsorbent and the adsorbate making hydrochloric acid unable to release the drug into the solution. Hydrogen bonds could also explain why the ionic strength of NaCl is also inefficient to remove the cationic pharmaceutical from the beads in addition to destroying the stability of the beads. As for MB, ethanol has little effect with van der Waals' interaction for the removal of famotidine because of the stability of hydrogen bonds.

The results for the desorption of diclofenac from the beads show that ethanol 1% v:v is able to release the pharmaceutical into solution. The percentages of desorption are high, around 70%, and the results present little difference between each kind of beads. Diclofenac is desorbed with NaOH 0.1 M from the beads mainly due to a change in the pH of the solution. As the results of the effect of pH showed, the adsorption of diclofenac was low in high pH solution. Like the other compounds, NaCl is not an efficient desorbent and damages the stability of the beads by interacting with the structure of the polymer.

4 Conclusion and perspectives

During this project, calcium alginate and calcium alginate/graphene oxide beads were evaluated as adsorbents for the removal of methylene blue, famotidine and diclofenac from aqueous solution.

The SEM analysis showed that an increase in graphene oxide modified the morphological structure of the beads. Indeed, they become more porous and rougher with a higher surface available for the interactions between adsorbate and adsorbent. As expected, during the adsorption process, Ca-Alg_2/GO20 beads present the best adsorption for each compound. The effect of initial concentration, adsorbent dose, pH and temperature all play an important role for the adsorption. The results show that a higher concentration of pharmaceuticals increases the diffusion driving force of drug adsorbed by the beads. With a lower concentration of beads, the adsorbed amount at equilibrium q_{eq} increases because of a higher amount adsorbed per unit of weight of the adsorbent. On the other hand, the percentage of removal decreases due to less adsorption sites available. The pH can modify the structure of the beads along with the pharmaceuticals causing a change in the interactions between adsorbate and adsorbent. The adsorption process is better at low temperature than high temperature meaning the adsorption mechanism is exothermic (as confirmed by H°) and thermodynamic studies show that the physisorption is spontaneous. The pseudo-second order model is the best fit to the experimental data concerning the kinetics of adsorption for methylene blue and famotidine, however the Lagergren pseudo-first order model suits better for diclofenac. Furthermore, each compound follows the Langmuir model for the isotherm adsorption with a maximum adsorption capacity of 1334, 35.50 and 36.35 $mg \cdot g^{-1}$ for methylene blue, famotidine and diclofenac, respectively. 0.1 M HCl and ethanol 1% v:v are efficient to desorb methylene blue and diclofenac, respectively, from the beads without damage to bead integrity, but further investigation needs to be performed for famotidine as little desorption is observed with the desorption candidates examined.

These beads appear to be an efficient adsorbent for dyes and pharmaceuticals, particularly for methylene blue. This novel technology could be applied in drinking or waste water treatment plants in order to reduce the concentration of these micro-pollutants which negatively impact the environment, human health and aquatic life. Methylene Blue is widely used a model pollutant in adsorption studies. It is interesting to note that while the performance of the beads assessed in this study is excellent for MB, it is less than stellar for FMTD and DFC. This calls into question the validity of the approach of single component pollutant for novel adsorbent testing.

5 Acknowledgments

I would like to thank all the people who supported and helped me during these three years in Sion at HES-SO Valais//Wallis. I also want to thank Professor Fabian Fischer and all my teachers who transmitted so much knowledge in an excellent environment.

I specially want to express my gratitude to Dr. Jenny Lawler, my supervisor, who gave me this huge opportunity to perform my Bachelor's thesis in Dublin City University.

I want to extend my thanks to everyone present in the lab to provide a nice atmosphere.

It was a great experience where I learned so much from different culture, different people. This is something I will always be grateful for and I will never forget.

6 Bibliography

[1] R.P. Schwarzenbach, B.I. Escher, K. Fenner, T.B. Hofstetter, C.A. Johnson, U. von Gunten, B. Wehrli, The Challenge of Micropollutants in Aquatic Systems, Science, 313 (2006) 1072.

[2] K. Fent, A.A. Weston, D. Caminada, Ecotoxicology of human pharmaceuticals, Aquatic Toxicology, 76 (2006) 122-159.

[3] K. Schirmer, M. Schirmer, Who is chasing whom? A call for a more integrated approach to reduce the load of micro-pollutants in the environment, Water Sci Technol, 57 (2008) 145-150.

[4] Alginic acid chemical structure, http://2012.igem.org/Team:Slovenia/SafetyMechanismsMicrocapsuleDegradation, (26.09.2016).

[5] G.T. Grant, E.R. Morris, D.A. Rees, P.J.C. Smith, D. Thom, Biological interactions between polysaccharides and divalent cations: The egg-box model, FEBS Letters, 32 (1973) 195-198.

[6] T. Chandy, D.L. Mooradian, G.H. Rao, Evaluation of modified alginate-chitosan-polyethylene glycol microcapsules for cell encapsulation, Artif Organs, 23 (1999) 894-903.

[7] O. Smidsrød, G. Skjâk-Braek, Alginate as immobilization matrix for cells, Trends in Biotechnology, 8 (1990) 71-78.

[8] W.M. Algothmi, N.M. Bandaru, Y. Yu, J.G. Shapter, A.V. Ellis, Alginate-graphene oxide hybrid gel beads: An efficient copper adsorbent material, Journal of Colloid and Interface Science, 397 (2013) 32-38.

[9] K.I. Draget, G. Skjåk Bræk, O. Smidsrød, Alginic acid gels: the effect of alginate chemical composition and molecular weight, Carbohydrate Polymers, 25 (1994) 31-38.

[10] S. Leick, S. Henning, P. Degen, D. Suter, H. Rehage, Deformation of liquid-filled calcium alginate capsules in a spinning drop apparatus, Physical Chemistry Chemical Physics, 12 (2010) 2950-2958.

[11] Structure of graphene oxide, http://www.greenoptimistic.com/graphene-oxide-offers-new-hope-for-water-decontamination-20130109/#.V-jpOLU44w4, (26.09.2016).

[12] Y. Zhu, S. Murali, W. Cai, X. Li, J.W. Suk, J.R. Potts, R.S. Ruoff, Graphene and graphene oxide: synthesis, properties, and applications, Adv Mater, 22 (2010) 3906-3924.

[13] E. Mitchell, A. Jimenez, R.K. Gupta, B.K. Gupta, K. Ramasamy, M. Shahabuddin, S.R. Mishra, Ultrathin porous hierarchically textured NiCo2O4-graphene oxide flexible nanosheets for high-performance supercapacitors, New Journal of Chemistry, 39 (2015) 2181-2187.

[14] Y.B. Tang, C.S. Lee, Z.H. Chen, G.D. Yuan, Z.H. Kang, L.B. Luo, H.S. Song, Y. Liu, Z.B. He, W.J. Zhang, I. Bello, S.T. Lee, High-quality Graphenes via a facile quenching method for field-effect transistors, Nano Lett, 9 (2009) 1374-1377.

[15] P.K. Ang, W. Chen, A.T. Wee, K.P. Loh, Solution-gated epitaxial graphene as pH sensor, J Am Chem Soc, 130 (2008) 14392-14393.

[16] X. Wang, L. Zhi, K. Mullen, Transparent, conductive graphene electrodes for dye-sensitized solar cells, Nano Lett, 8 (2008) 323-327.

[17] X. Deng, L. Lu, H. Li, F. Luo, The adsorption properties of Pb(II) and Cd(II) on functionalized graphene prepared by electrolysis method, J Hazard Mater, 183 (2010) 923-930.

[18] X. Wang, Z. Liu, X. Ye, K. Hu, H. Zhong, J. Yu, M. Jin, Z. Guo, A facile one-step approach to functionalized graphene oxide-based hydrogels used as effective adsorbents toward anionic dyes, Applied Surface Science, 308 (2014) 82-90.

[19] S. Wu, X. Zhao, Y. Li, Q. Du, J. Sun, Y. Wang, X. Wang, Y. Xia, Z. Wang, L. Xia, Adsorption Properties of Doxorubicin Hydrochloride onto Graphene Oxide: Equilibrium, Kinetic and Thermodynamic Studies, Materials, 6 (2013) 2026-2042.

[20] L. Chen, P. Hu, L. Zhang, S. Huang, L. Luo, C. Huang, Toxicity of graphene oxide and multi-walled carbon nanotubes against human cells and zebrafish, Science China Chemistry, 55 (2012) 2209-2216.

[21] Y.S. Jeon, J. Lei, J.-H. Kim, Dye adsorption characteristics of alginate/polyaspartate hydrogels, Journal of Industrial and Engineering Chemistry, 14 (2008) 726-731.

[22] Structure of MB, https://commons.wikimedia.org/wiki/File:Methylene_blue.svg, (26.09.2016).

[23] A.F. Hassan, A.M. Abdel-Mohsen, M.M.G. Fouda, Comparative study of calcium alginate, activated carbon, and their composite beads on methylene blue adsorption, Carbohydrate Polymers, 102 (2014) 192-198.

[24] B. Yasemin, A. Haluk, A kinetics and thermodynamics study of methylene blue adsorption on wheat shells, Desalination, 194 (2006) 259–267.

[25] E.N. El Qada, S.J. Allen, G.M. Walker, Adsorption of Methylene Blue onto activated carbon produced from steam activated bituminous coal: A study of

equilibrium adsorption isotherm, Chemical Engineering Journal, 124 (2006) 103-110.

[26] M.N. Ahmed, R.N. Ram, Removal of basic dye from waste-water using silica as adsorbent, Environmental Pollution, 77 (1992) 79-86.

[27] A.K. Mittal, C. Venkobachar, Studies on sorption of dyes by sulfonated coal and Ganoderma lucidum, Indian Journal of Environmental Health, 31 (2) (1989) 105–111.

[28] Structure of famotidine, https://dailymed.nlm.nih.gov/dailymed/archives/fdaDrugInfo.cfm?archiveid=2974, (26.09.2016).

[29] J.C. Breitner, K.A. Welsh, M.J. Helms, P.C. Gaskell, B.A. Gau, A.D. Roses, M.A. Pericak-Vance, A.M. Saunders, Delayed onset of Alzheimer's disease with nonsteroidal anti-inflammatory and histamine H2 blocking drugs, Neurobiol Aging, 16 (1995) 523-530.

[30] S.P. Molinari, R. Kaminski, A. Di Rocco, M.D. Yahr, The use of famotidine in the treatment of Parkinson's disease: a pilot study, J Neural Transm Park Dis Dement Sect, 9 (1995) 243-247.

[31] M. Gros, M. Petrovic, A. Ginebreda, D. Barcelo, Removal of pharmaceuticals during wastewater treatment and environmental risk assessment using hazard indexes, Environ Int, 36 (2010) 15-26.

[32] J.-W. Kim, H. Ishibashi, R. Yamauchi, N. Ichikawa, Y. Takao, M. Hirano, M. Koga, K. Arizono, Acute toxicity of pharmaceutical and personal care products on freshwater crustacean (Thamnocephalus platyurus) and fish (Oryzias latipes), The Journal of Toxicological Sciences, 34 (2009) 227-232.

[33] N. Bhala, J. Emberson, A. Merhi, S. Abramson, N. Arber, Vascular and upper gastrointestinal effects of non-steroidal anti-inflammatory drugs: meta-analyses of individual participant data from randomised trials, Lancet, 382 (2013) 769-779.

[34] R. Altman, B. Bosch, K. Brune, P. Patrignani, C. Young, Advances in NSAID Development: Evolution of Diclofenac Products Using Pharmaceutical Technology, Drugs, 75 (2015) 859-877.

[35] Structure of diclofenac, https://fr.wikipedia.org/wiki/Diclof%C3%A9nac#/media/File:Diclofenac.svg, (26.09.2016).

[36] R. Triebskorn, H. Casper, A. Heyd, R. Eikemper, H.R. Köhler, J. Schwaiger, Toxic effects of the non-steroidal anti-inflammatory drug diclofenac: Part II. Cytological effects in liver, kidney, gills and intestine of rainbow trout (Oncorhynchus mykiss), Aquatic Toxicology, 68 (2004) 151-166.

[37] R. Triebskorn, H. Casper, V. Scheil, J. Schwaiger, Ultrastructural effects of pharmaceuticals (carbamazepine, clofibric acid, metoprolol, diclofenac) in rainbow trout (Oncorhynchus mykiss) and common carp (Cyprinus carpio), Anal Bioanal Chem, 387 (2007) 1405-1416.

[38] Y.M. Slokar, A. Majcen Le Marechal, Methods of decoloration of textile wastewaters, Dyes and Pigments, 37 (1998) 335-356.

[39] T.A. Ternes, M. Meisenheimer, D. McDowell, F. Sacher, H.J. Brauch, B. Haist-Gulde, G. Preuss, U. Wilme, N. Zulei-Seibert, Removal of pharmaceuticals during drinking water treatment, Environ Sci Technol, 36 (2002) 3855-3863.

[40] J. Radjenovic, M. Petrovic, D. Barceló, Analysis of pharmaceuticals in wastewater and removal using a membrane bioreactor, Analytical and Bioanalytical Chemistry, 387 (2007) 1365-1377.

[41] G.Z. Kyzas, E.A. Deliyanni, K.A. Matis, Graphene oxide and its application as an adsorbent for wastewater treatment, Journal of Chemical Technology & Biotechnology, 86 (2) (2013) 196-205.

[42] I. Langmuir, The constitution and fundamental properties of solids and liquids, Journal of the Franklin Institute, 183 (1917) 102-105.

[43] H. Freundlich, Über die Adsorption in Lösungen, W. Engelmann 1906.

[44] T. Liu, Y. Li, Q. Du, J. Sun, Y. Jiao, G. Yang, Z. Wang, Y. Xia, W. Zhang, K. Wang, H. Zhu, D. Wu, Adsorption of methylene blue from aqueous solution by graphene, Colloids and Surfaces B: Biointerfaces, 90 (2012) 197-203.

[45] R. Aravindhan, N.N. Fathima, J.R. Rao, B.U. Nair, Equilibrium and thermodynamic studies on the removal of basic black dye using calcium alginate beads, Colloids and Surfaces A: Physicochemical and Engineering Aspects, 299 (2007) 232-238.

[46] S.R. Popuri, Y. Vijaya, V.M. Boddu, K. Abburi, Adsorptive removal of copper and nickel ions from water using chitosan coated PVC beads, Bioresource Technology, 100 (2009) 194-199.

[47] B.H. Hameed, Evaluation of papaya seeds as a novel non-conventional low-cost adsorbent for removal of methylene blue, Journal of Hazardous Materials, 162 (2009) 939-944.

[48] Y. Li, F. Liu, B. Xia, Q. Du, P. Zhang, D. Wang, Z. Wang, Y. Xia, Removal of copper from aqueous solution by carbon nanotube/calcium alginate composites, Journal of Hazardous Materials, 177 (2010) 876-880.

[49] V. Rocher, J.-M. Siaugue, V. Cabuil, A. Bee, Removal of organic dyes by magnetic alginate beads, Water Research, 42 (2008) 1290-1298.

[50] V. Vadivelan, K.V. Kumar, Equilibrium, kinetics, mechanism, and process design for the sorption of methylene blue onto rice husk, Journal of Colloid and Interface Science, 286 (2005) 90-100.

[51] F.J. Beltrán, P. Pocostales, P. Alvarez, A. Oropesa, Diclofenac removal from water with ozone and activated carbon, Journal of Hazardous Materials, 163 (2009) 768-776.

[52] S.-W. Nam, C. Jung, H. Li, M. Yu, J.R.V. Flora, L.K. Boateng, N. Her, K.-D. Zoh, Y. Yoon, Adsorption characteristics of diclofenac and sulfamethoxazole to graphene oxide in aqueous solution, Chemosphere, 136 (2015) 20-26.

[53] Y. Li, Q. Du, T. Liu, J. Sun, Y. Wang, S. Wu, Z. Wang, Y. Xia, L. Xia, Methylene blue adsorption on graphene oxide/calcium alginate composites, Carbohydrate Polymers, 95 (2013) 501-507.

[54] M.R. Reddy, S.J. Dunn, Distribution coefficients for nickel and zinc in soils, Environmental Pollution Series B, Chemical and Physical, 11 (1986) 303-313.

[55] P.C. Gomes, M.P.F. Fontes, A.G. da Silva, E. de S. Mendonça, A.R. Netto, Selectivity Sequence and Competitive Adsorption of Heavy Metals by Brazilian Soils, Soil Science Society of America Journal, 65 (2001) 1115-1121.

[56] L.A. Al-Khateeb, S. Almotiry, M.A. Salam, Adsorption of pharmaceutical pollutants onto graphene nanoplatelets, Chemical Engineering Journal, 248 (2014) 191-199.

[57] A.N. Fernandes, C.A.P. Almeida, N.A. Debacher, M.M.d.S. Sierra, Isotherm and thermodynamic data of adsorption of methylene blue from aqueous solution onto peat, Journal of Molecular Structure, 982 (2010) 62-65.

[58] C.H. Weng, Y.T. Lin, T.W. Tzeng, Removal of methylene blue from aqueous solution by adsorption onto pineapple leaf powder, J Hazard Mater, 170 (2009) 417-424.

[59] Y. Yu, Y.-Y. Zhuang, Z.-H. Wang, Adsorption of Water-Soluble Dye onto Functionalized Resin, Journal of Colloid and Interface Science, 242 (2001) 288-293.

[60] P. Wang, M. Cao, C. Wang, Y. Ao, J. Hou, J. Qian, Kinetics and thermodynamics of adsorption of methylene blue by a magnetic graphene-carbon nanotube composite, Applied Surface Science, 290 (2014) 116-124.

[61] I.D. Mall, V.C. Srivastava, N.K. Agarwal, Removal of Orange-G and Methyl Violet dyes by adsorption onto bagasse fly ash—kinetic study and equilibrium isotherm analyses, Dyes and Pigments, 69 (2006) 210-223.

[62] K.K. Panday, G. Prasad, V.N. Singh, Mixed adsorbent for Cu(II) removal from aqueous solutions, Environ Technol Lett, 7 (1986) 547-554.

[63] J. Ma, Y. Jia, Y. Jing, Y. Yao, J. Sun, Kinetics and thermodynamics of methylene blue adsorption by cobalt-hectorite composite, Dyes and Pigments, 93 (2012) 1441-1446.

[64] N. Kannan, M.M. Sundaram, Kinetics and mechanism of removal of methylene blue by adsorption on various carbons—a comparative study, Dyes and Pigments, 51 (2001) 25-40.

[65] S.K. Bajpai, M. Bhowmik, - Adsorption of diclofenac sodium from aqueous solution using polyaniline as a potential sorbent. I. Kinetic studies, - Journal of Applied Polymer Science, 117 (2010) 3615-3622.

[66] S.-T. Yang, S. Chen, Y. Chang, A. Cao, Y. Liu, H. Wang, Removal of methylene blue from aqueous solution by graphene oxide, Journal of Colloid and Interface Science, 359 (2011) 24-29.

[67] G. McKay, J.F. Porter, G.R. Prasad, The removal of dye colours from aqueous solutions by adsorption on low-cost materials, Water Air Soil Pollut. 114 (1999) 423–438.

[68] J.X. Yu, B.H. Li, X.M. Sun, J. Yuan, R.A. Chi, Polymer modified biomass of baker's yeast for enhancement adsorption of methylene blue, rhodamine B and basic magenta, J. Hazard. Mater. 168 (2009) 1147–1154.

[69] J.X. Yu, B.H. Li, X.M. Sun, J. Yuan, R.A. Chi, Poly(amic acid)-modified biomass of baker's yeast for enhancement adsorption of methylene blue and basic magenta, Appl Biochem Biotechnol, 160 (2010) 1394-1406.

[70] E.N. El Qada, S.J. Allen, G.M. Walker, Adsorption of basic dyes from aqueous solution onto activated carbons, Chem. Eng. J. 135 (2008) 174–184.

[71] J. Yamashita, M. Shioya, T. Kikutani, T. Hashimoto, Activated carbon fibers and films derived from poly(vinylidene fluoride), Carbon 39 (2001) 207– 214.

[72] B.H. Hameed, Grass waste: a novel sorbent for the removal of basic dye from aqueous solution, J. Hazard. Mater. 166 (2009) 233–238.

[73] B.H. Hameed, A.T.M. Din, A.L. Ahmad, Adsorption of methylene blue onto bamboo-based activated carbon: kinetics and equilibrium studies, J. Hazard. Mater. 141 (2007) 819–825.

[74] K. Legrouri, E. Khouyab, M. Ezzinea, H. Hannachea, R. Denoyelc, R. Pallierd, R. Naslaind, Production of activated carbon from a new precursor molasses by activation with sulphuric acid, J. Hazard. Mater. B118 (2005) 259–263.

[75] I.A.W. Tan, A.L. Ahmad, B.H. Hameed, Adsorption of basic dye on high-surface-area activated carbon prepared from coconut husk: equilibrium, kinetic and thermodynamic studies, J. Hazard. Mater. 154 (2008) 337–346.

[76] S. Altenor, B. Carene, E. Emmanuel, J. Lambert, J.J. Ehrhardt, S. Gaspard, Adsorp- tion studies of methylene blue and phenol onto vetiver roots activated carbon prepared by chemical activation, J. Hazard. Mater. 165 (2009) 1029–1039.

[77] K. Marungrueng, P. Pavasant, High performance biosorbent (Caulerpa lentillifera) for basic dye removal, Bioresour. Technol. 98 (2007) 1567– 1572.

[78] A.A. Attia, B.S. Girgis, N.A. Fathy, Removal of methylene blue by carbons derived from peach stones by H3PO4 activation: batch and column studies, Dyes Pigments 76 (2008) 282–289.

[79] K.V. Kumar, S. Sivanesan, Equilibrium data, isotherm parameters and process design for partial and complete isotherm of methylene blue onto activated carbon, J. Hazard. Mater. 134 (2006) 237–244.

[80] B.H. Hameed, I.A.W. Tan, A.L. Ahmad, Optimization of basic dye removal by oil palm fibre-based activated carbon using response surface methodology, J. Hazard. Mater. 158 (2008) 324–332.

[81] B.H. Hameed, D.K. Mahmoud, A.L. Ahmad, Sorption of basic dye from aqueous solution by pomelo (Citrus grandis) peel in a batch system, Colloids Surf. A316 (2008) 78–84.

[82] A.N. Fernandes, C.A.P. Almeida, C.T.B. Menezes, N.A. Debacher, M.M.D. Sierra, Removal of methylene blue from aqueous solution by peat, J. Hazard. Mater. 144 (2007) 412–419.

[83] M. Bagane, S. Guiza, Removal of a dye from textile effluents by adsorption, Ann. Chim. 25 (2000) 615–626.

[84] C.A.P. Almeida, N.A. Debacher, A.J. Downs, L. Cottet, C.A.D. Mello, Removal of methylene blue from colored effluents by adsorption on montmorillonite clay, J. Colloid Interface Sci. 332 (2009) 46–53.

[85] E. Rubin, P. Rodriguez, R. Herrero, J. Cremades, I. Barbara, M.E. Sastre de Vicente, Removal of methylene blue from aqueous solutions using as biosorbent Sargassum muticum: an invasive macroalga in Europe, J. Chem. Technol. Biotechnol. 80 (2005) 291–298.

[86] M.C. Ncibi, A.M.B. Hamissa, A. Fathallah, M.H. Kortas, T. Baklouti, B. Mahjoub, M. Seffen, Biosorptive uptake of methylene blue using Mediterranean green alga Enteromorpha spp., J. Hazard. Mater. 170 (2009) 1050–1055.

[87] M.A. Al-Ghouti, M.A.M. Khraisheh, S.J. Allen, M.N. Ahmad, The removal of dyes from textile wastewater: a study of the physical characteristics and adsorption mechanisms of diatomaceous earth, J. Environ. Manage. 69 (2003) 229–238.

[88] M. Dogan, M. Alkan, Y. Onager, Adsorption of methylene blue from aqueous solution onto perlite, Water Air Soil Pollut. 120 (2000) 229–248.

[89] Keane, D. 2013. Evaluation of the performance of activated carbon and titanium dioxide composites for pharmaceutical adsorption and photocatalysis in water. PhD thesis. Dublin City University.

[90] R. Baccar, M. Sarrà, J. Bouzid, M. Feki, P. Blánquez, Removal of pharmaceutical compounds by activated carbon prepared from agricultural by-product, Chemical Engineering Journal, 211–212 (2012) 310-317.

[91] X. Hu, Z. Cheng, Removal of diclofenac from aqueous solution with multi-walled carbon nanotubes modified by nitric acid, Chinese Journal of Chemical Engineering, 23 (2015) 1551-1556.

[92] S. Jodeh, F. Abdelwahab, N. Jaradat, I. Warad, W. Jodeh, Adsorption of diclofenac from aqueous solution using Cyclamen persicum tubers based activated carbon (CTAC), Journal of the Association of Arab Universities for Basic and Applied Sciences, 20 (2016) 32-38.

[93] Q. Tang, N. Yu, Z. Li, D. Wu, Y. Sun, J. Abdelhamid Sayari and Mietek, Famotidine drug adsorption on carboxylic acid functionalized ordered SBA-15 mesoporous silica, Studies in Surface Science and Catalysis, Elsevier2005, pp. 649-656.

[94] H. Ahmad Panahi, S. Nasrollahi, Polymer brushes containing thermosensitive and functional groups grafted onto magnetic nano-particles for interaction and extraction of famotidine in biological samples, International Journal of Pharmaceutics, 476 (2014) 70-76.

[95] Q. Tang, Y. Xu, D. Wu, Y. Sun, A study of carboxylic-modified mesoporous silica in controlled delivery for drug famotidine, Journal of Solid State Chemistry, 179 (2006) 1513-1520.

[96] W. Xu, Q. Gao, Y. Xu, D. Wu, Y. Sun, W. Shen, F. Deng, Controlled drug release from bifunctionalized mesoporous silica, Journal of Solid State Chemistry, 181 (2008) 2837-2844.

[97] T. De Oliveira, R. Guégan, T. Thiebault, C.L. Milbeau, F. Muller, V. Teixeira, M. Giovanela, M. Boussafir, Adsorption of diclofenac onto organoclays: Effects of surfactant and environmental (pH and temperature) conditions, Journal of Hazardous Materials.

[98] M.D. Vedenyapina, D.A. Borisova, A.P. Simakova, L.P. Proshina, A.A. Vedenyapin, Adsorption of diclofenac sodium from aqueous solutions on expanded graphite, Solid Fuel Chemistry, 47 (2013) 59-63.

[99] Z. Hasan, N.A. Khan, S.H. Jhung, Adsorptive removal of diclofenac sodium from water with Zr-based metal–organic frameworks, Chemical Engineering Journal, 284 (2016) 1406-1413.

[100] S. Larous, A.-H. Meniai, Adsorption of Diclofenac from aqueous solution using activated carbon prepared from olive stones, International Journal of Hydrogen Energy, 41 (2016) 10380-10390.

[101] B.N. Bhadra, P.W. Seo, S.H. Jhung, Adsorption of diclofenac sodium from water using oxidized activated carbon, Chemical Engineering Journal, 301 (2016) 27-34.

[102] M. Antunesa, V.I. Esteves, R. Guégan, J.S. Crespo, A.N. Fernandes, M. Giovanela, Removal of diclofenac sodium from aqueous solution by Isabel grape bagasse, Chem. Eng. J. 192 (2012) 114–121.

[103] C. Saucier, M.A. Adebayo, E.C. Lima, R. Cataluna, P.S. Thue, L.D. T. Prola, M.J. Puchana-Rosero, F. M. Machado, F.A. Pavan, G.L. Dotto, Microwave-assisted activated carbon from cocoa shell as adsorbent for removal of sodium diclofenac and nimesulide from aqueous effluents, J. Hazard. Mater. 289 (2015) 18–27.

[104] P. Sathishkumar, M. Arulkumar, V. Ashokkumar, A.R. Mohd Yusoff, K. Murugesan, T. Palvannan, Z. Salam, F.N. Ani, T. Hadibarata, Modified phyto-waste Terminalia catappa fruit shells: a reusable adsorbent for the removal of micropollutant diclofenac, RSC Advances, 5 (2015) 30950-30962.

[105] H. Wei, S. Deng, Q. Huang, Y. Nie, B. Wang, J. Huang, G. Yu, Regenerable granular carbon nanotubes/alumina hybrid adsorbents for diclofenac sodium and carbamazepine removal from aqueous solution, Water Research, 47 (2013) 4139-4147.

7 Appendix

Appendix I

Pictures of Ca-Alg_2 (A), Ca-Alg_2/GO5 (B), Ca-Alg_2/GO10 (C), Ca-Alg_2/GO20 (D) wet and dried beads.

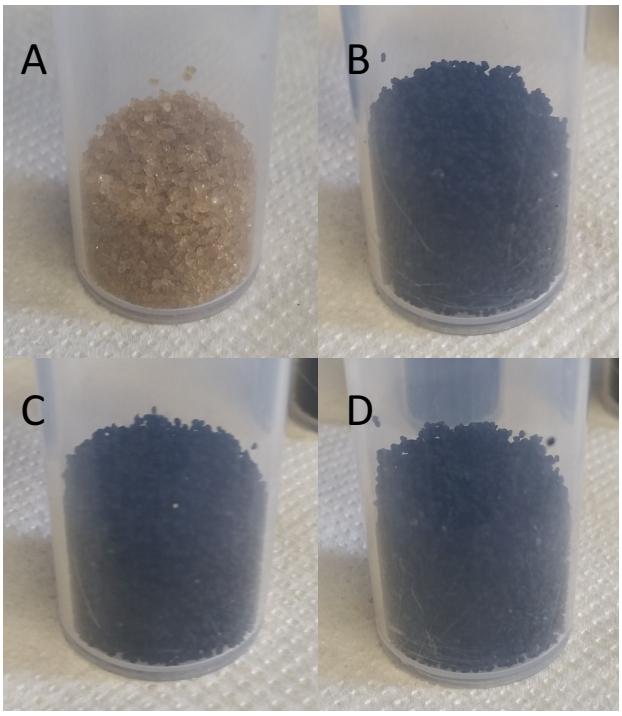

Appendix II

SEM images of Ca--Alg_2 (A), Ca-Alg_2/GO5 (B), Ca-Alg_2/GO10 (C), Ca-Alg_2/GO20 (D) beads with a magnification of 100 and 2500 times.

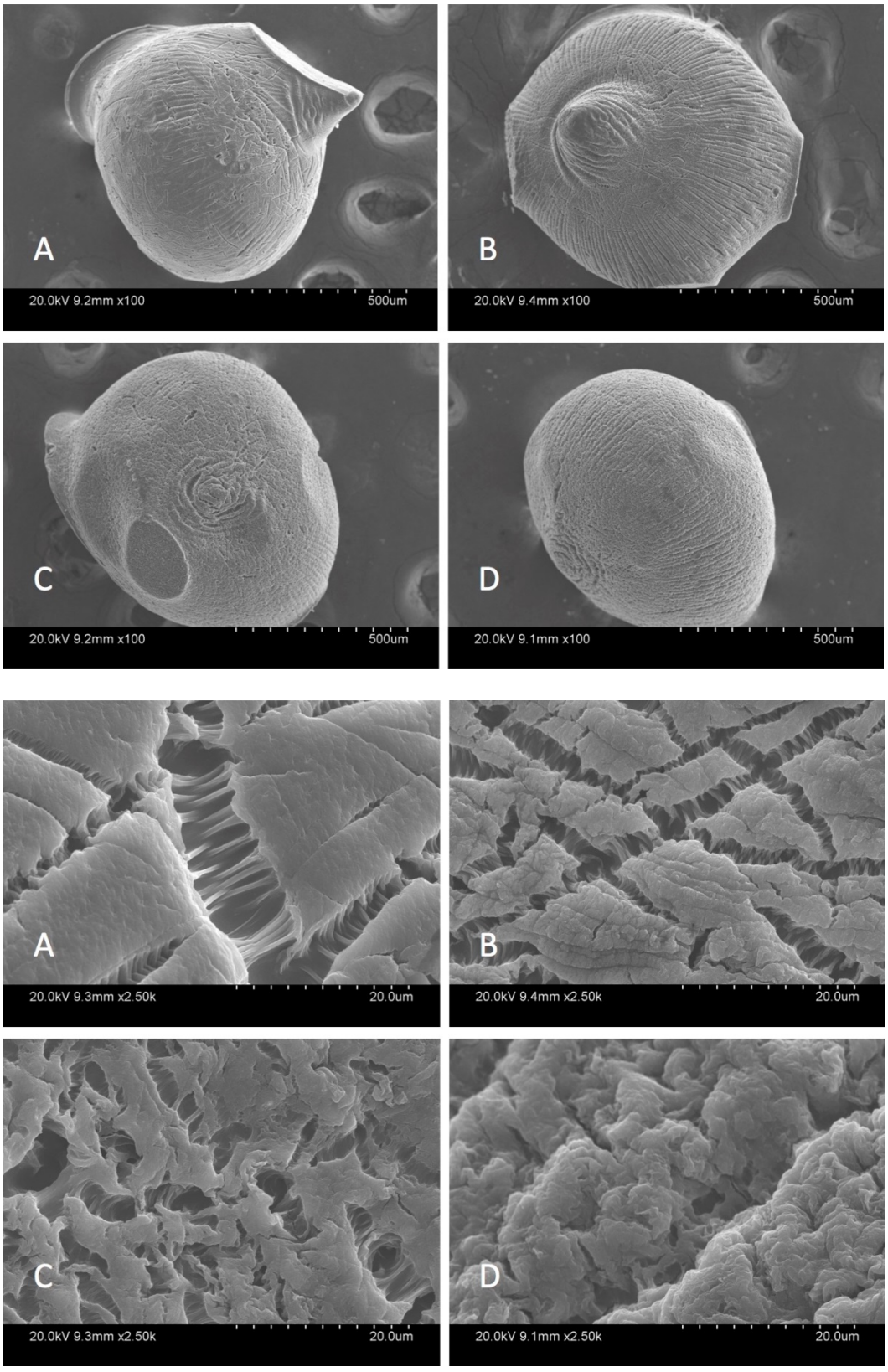

Appendix III

Calibration curves for methylene blue.

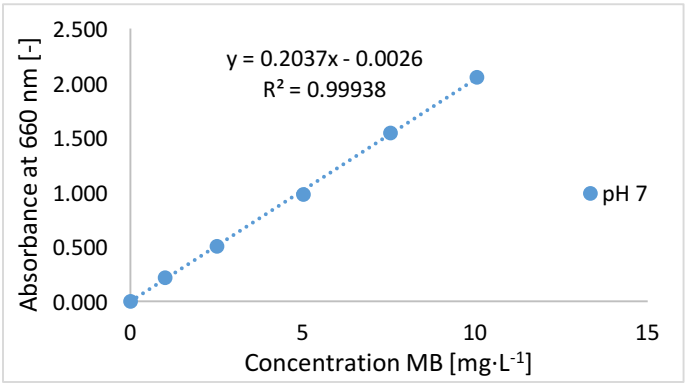

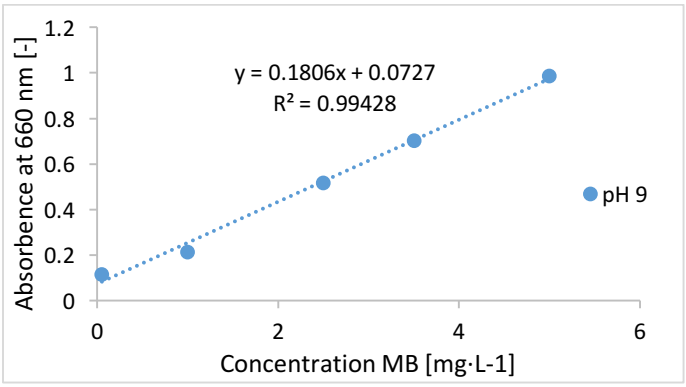

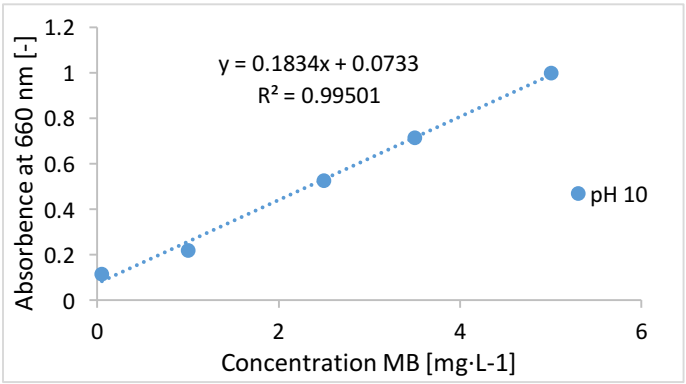

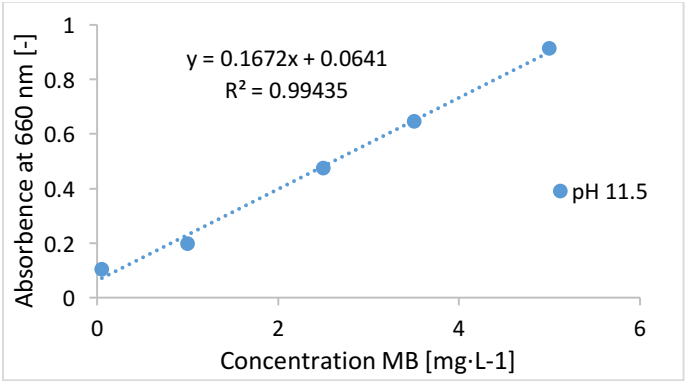

Calibration curves for famotidine.

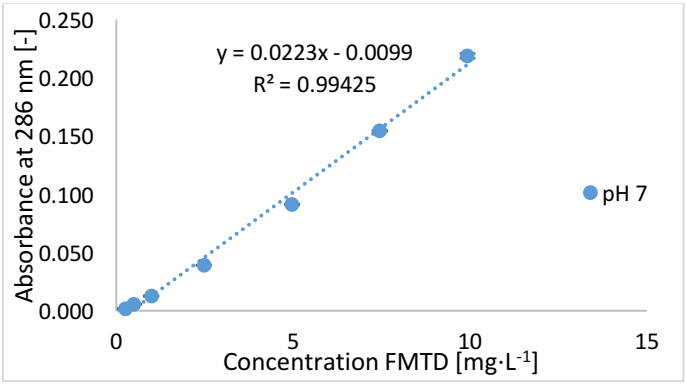

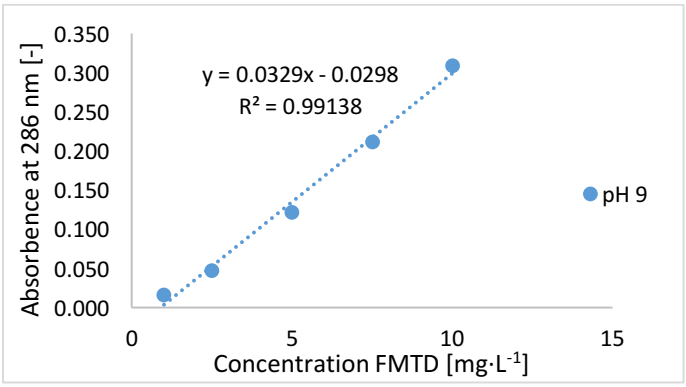

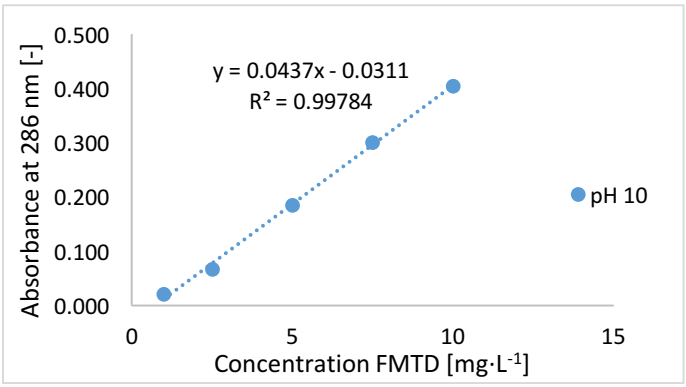

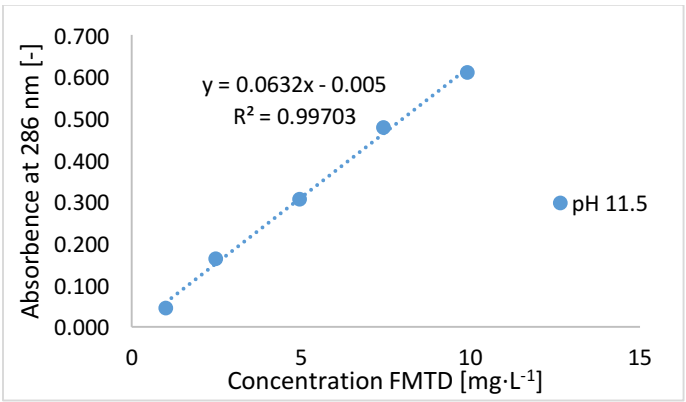

Calibration curves for diclofenac.